Australian Government
Department of Defence
Science and Technology

Thoraco-abdominal Organ Locations: Variations due to Breathing and Posture and Implications for Body Armour Coverage Assessments

Sheridan Laing and Mark Jaffrey

Land Division
Defence Science and Technology Group

DST-Group-TR-3636

ABSTRACT

Body armour provides protection to the vital organs and structures of the thorax and abdomen against ballistic, stab and fragmentation threats. The positions of the organs and structures determine the coverage requirements and hence the required dimensions of body armour. The aim of this study was to quantify thoraco-abdominal organ and structure boundaries for varied breathing and postural conditions and develop a preliminary database for use in body armour coverage analyses. This Technical Report documents the methodological details of the study and reports the descriptive statistics of the anatomical data. The data herein shows the necessity for consideration of breathing and postural conditions that can substantially affect the required dimensions of body armour coverage. The data may be used to establish a preliminary representative population database of thoraco-abdominal anatomical structure boundary positions with respect to the studied breathing and postural conditions. Such a database will facilitate more evidence-based design and assessment of the coverage afforded by body armour.

RELEASE LIMITATION

Approved for public release

Produced by

Land Division
Defence Science and Technology Group
506 Lorimer St
Fishermans Bend, Victoria 3207 Australia

Telephone: 1300 333 362

August 2019

APPROVED FOR PUBLIC RELEASE

Thoraco-abdominal Organ Locations: Variations due to Breathing and Posture and Implications for Body Armour Coverage Assessments

Executive Summary

Body armour is used by police and military personnel to provide passive protection of the vital organs of the thorax and abdomen against ballistic, fragmentation and stab threats. Optimising the amount of coverage provided by body armour requires consideration of the trade-off between the passive protection afforded by the armour and its potential to hinder wearers' ability to actively protect themselves. Although body armour is available in a range of sizes and dimensions, there is a dearth of quantitative data in the literature regarding the absolute locations of the organs and anatomical structures for which coverage is required. Thus, the ability to evaluate the coverage provided by body armour is limited. Furthermore, changes to breathing and posture are hypothesised to result in changes in organ positioning and hence coverage requirements.

The aim of this study was to quantify the positions of internal thoraco-abdominal organs and structures relative to an external anthropometric landmark, for a cohort of young male adults and to quantify the effects of breathing and postural changes. MRI scanning was conducted in three scan conditions: supine expiration, supine inspiration and upright with shallow breathing near expiration.

The lateral boundaries of organs determine the width requirements of body armour. Inspiration resulted in the most lateral organ boundaries with the exception of the heart. The left cardiac boundary was more laterally positioned during expiration. The upright condition generally resulted in the most inferior organ boundaries, representing the most conservative locations for body armour length analysis. The upright condition also represents a common posture adopted by police and military personnel. Thus the upright data was used for an exemplar body armour coverage analysis. Furthermore, parametrised distributions of the upright organ boundary data have been presented for use in simple coverage analysis of existing or proposed body armour dimensions.

This report documents the methodological detail of the study and provides a preliminary database of organ boundary coverage data for use in body armour coverage analyses. The data herein shows the necessity for consideration of breathing and postural conditions which can substantially affect the required dimensions of body armour coverage. This initial study heralds a significant step in establishing a representative population database of thoraco-abdominal anatomical structure boundary positions that will facilitate more evidence-based design and assessment of the passive protection afforded by body armour.

This page is intentionally blank.

Authors

Sheridan Laing

Land Division

Sheridan holds a Bachelor of Biomedical Engineering and is currently completing a PhD in Biomechanics at the University of Melbourne. Since joining DST in 2012, Sheridan's work has concentrated on the analysis of traumatic injuries and human vulnerability, providing injury biomechanics support to the Australian Army in the assessment of soldier systems in dismounted and mounted environments.

Mark Jaffrey

Land Division

Mark has been employed with the Defence Science and Technology Group since 2001. He has a PhD in biomechanics from Victoria University. Mark works in the areas of injury biomechanics, combat casualty analysis and protective systems performance assessment. He is currently leading the physical and physiological performance research capability in Land Division of DST Group.

This page is intentionally blank

Contents

This page is intentionally blank.

1. Introduction

Body armour is used by police and military personnel to provide passive protection of the vital organs of the thorax and abdomen against ballistic, fragmentation and stab threats. Current body armour solutions fall into one of two categories, referred to herein as soft armour and hard plates. Soft armour materials, such as aramid-based products, are used to provide protection against stab and low velocity ballistic threats, such as those from handguns and some explosive fragments. Hard plates, often constructed of ceramic material, are generally worn over soft armour and are used to provide protection against higher velocity ballistic threats. Although body armour provides passive protection, it can also reduce wearers' ability to actively protect themselves by introducing a mass burden and human-system integration issues. Such issues may reduce wearers' mobility, ability to rapidly take cover, and their capacity to carry out essential lethality tasks, such as sighting and firing a weapon (1-3).

Optimising the amount of coverage provided by body armour requires consideration of the trade-off between the passive protection afforded by the armour and its potential to hinder wearers' ability to actively protect themselves. Evidence-based design and fitting of the armour requires knowledge of the locations of the organs and anatomical structures for which coverage is required or desired.

Existing descriptions of body armour coverage requirements are largely qualitative in nature. Coverage requirements differ depending on the intended use and anticipated threats that the wearer may face. Body armour standards for UK police state that ballistic and stab resistant armour must provide coverage to the "major organs", defined as the heart, liver, lungs, kidneys and spleen (4). The National Institute of Justice (NIJ) stab resistant armour standard states that the protected area must ensure coverage of the "vital organs", defined as the heart, liver, spine, kidneys and spleen (5). No rationale for the aforementioned requirements is given within the respective standards.

Through a systematic review of literature, Breeze et al. identified the anatomical structures of the thorax and abdomen for which body armour coverage was required, categorising the identified structures as either "essential" or "desirable" (6). Coverage was deemed essential for those structures which, if damaged, would likely lead to death within 60 minutes of injury. Coverage was deemed desirable for those anatomical structures which, if damaged, would result in significant long-term morbidity. Anatomical structures requiring essential coverage were identified as the heart, the great vessels (the aorta, pulmonary arteries and veins and the venae cavae), the liver and the spleen. It was recommended these structures are covered by a hard plate. The lungs, thoraco-lumbar spinal cord, kidneys and intestines were identified as desirable for coverage. Soft armour coverage was recommended for these structures.

Breeze et al. also investigated the dimensions of body armour required to provide essential and desirable medical coverage as defined (7). The boundaries of the organs and structures of interest were identified using computed tomography (CT) scans of 120 Caucasian UK Armed Forces personnel. The CT scans were collected from injured service personnel on

hospital admission as part of the trauma call protocol and were analysed retrospectively. Data presented includes the lengths and widths of essential organs, the horizontal and vertical distances between anatomical structures and the distances between bone landmarks and the underlying anatomical structures. Relationships between selected vertical anthropometric measures and the dimensions of required coverage were also explored. The study by Breeze et al. forms the largest and most detailed information regarding the dimensions for body armour coverage currently available (7). However, the study is limited by the lack of breathing control of the participants and the recumbent nature of the scans.

Recently, the development of multi-positional magnetic resonance imaging (MRI) technology has facilitated imaging of thoraco-abdominal organs in an upright position, albeit at a lower resolution than conventional recumbent MRI. This technology has been utilised for the increased fidelity of human models for automotive uses (8, 9), however it is yet to be used for human vulnerability models for ballistic or stab threat analysis. Previous studies investigating organ movement from supine to upright (seated or standing) positions have focussed on the movement of the liver, spleen and kidneys. Organ movement was primarily observed in the superior-inferior directions, where organs moved inferiorly as the torso is positioned upright (8-11). The largest sample utilised in these studies was nine participants (8) and in each of the listed studies movement was described using the centre of gravity (CoG) of the organs. Thus, this information is of little use in describing the body armour dimensions required to cover the boundaries of organs in an upright posture.

The use of ultrasound imaging also permits anatomical data capture in an upright posture. Bleetman and Dyer measured the length of the exposed parts of the pericardium, liver, spleen and kidneys beneath the lower costal margin using ultrasound with upright participants (12). The inferior boundaries of the stated organs were measured for twenty-five participants (fifteen males and ten females) at full inspiration. However, this data cannot be used in assessing body armour coverage as minimal detail is provided on the techniques of the measurement and the reference frame for the provided values is unclear.

The aim of this study was to develop a database of internal thoraco-abdominal organ and structure boundaries for use in body armour coverage analyses with consideration of the influences of breathing and postural changes. This Technical Report aims to make available the methodological details of the study and report the descriptive statistics of the anatomical data. The effects of breathing and posture on the positions of the anatomical structures were investigated to understand the necessity for consideration of these conditions and exemplar body armour coverage assessments were conducted using common hard armour plate dimensions stated in the literature. The data herein may be used to establish a representative population database of thoraco-abdominal anatomical structure boundary positions with respect to the studied breathing and postural conditions. Such a database will facilitate more evidence-based design and assessment of the coverage afforded by body armour.

2. Methods

2.1. Participants

Twenty-five male participants between the ages of 20 and 42 (mean 29.2 ± 6.3 years) were recruited for the study. Ten were active members of the Australian Army, aged between 24 and 32 years. Fifteen civilian participants were recruited to ensure a broader age spectrum which better represents the Australian Army population (13). Ethical approval to conduct the study was granted in accordance with the DST Group low risk human research ethics review process (protocol LD 10-13).

Prior to participation, participants underwent basic medical and health screening, which included age, height, and weight measurements and screening for conditions which may affect the participants' ability to safely undergo MRI, including any history of claustrophobia, presence of metallic implants, and a history of welding, grinding or metal work or gunshot/shrapnel injuries. Due to inconsistencies in the breathing techniques adopted by two participants, only the data of 23 males has been utilised in the conducted analyses thus far.

2.2. Anthropometric measures

The following fifteen measures were recorded for each participant: cervical height, T2 height, sternal notch (SN) height, substernal height, 10th Rib height, iliac crest (IC) height, chest breadth, chest depth, chest circumference, waist circumference, back length, thelion-thelion distance, stature, sitting height and weight. The participants' front length was calculated as the SN height minus the IC height. All anthropometric measurements were taken in accordance with the methods used in the Australian Warfighter Anthropometric Survey (AWAS) (13, 14) and with the exception of the sitting height measurement, the participants were standing for all measures.

2.3. Magnetic Resonance Imaging

Three scan types were taken to capture organ size/position variation due to changes in breathing and postural conditions. Breathing conditions were investigated using a traditional recumbent MRI scanner, and an upright scanner was used to determine the effect of changes in postural conditions (i.e. recumbent vs. upright). Due to availability limitations, only 14 of the 23 participants underwent scanning with the upright scanner. The participants were instructed to remain as still as possible while in the machine. The scan parameters for each MRI machine were chosen to optimise the resolution and contrast between the soft internal organs of the thoraco-abdominal region (Table 2-1). No cardiac gating was used on any scans. Fiduciary markers consisting of fish oil capsules or almonds were taped to the participants as points of reference in the medical images. The markers were positioned with the participant in the posture corresponding to the scans being performed (supine or upright), thus accounting for skin movement artefact.

Table 2-1 Scan parameters used for recumbent and upright MRIs

MRI Machine	Field Strength (T)	Scan plane	Scan type	Slice thickness (mm)	Space between slices (mm)	Pixel dimensions^ (x/y) (mm)
Recumbent	3.0	Coronal	T1FFE	3.6	1.8	0.875/0.875
Upright	0.6	Coronal	T2FSE	6.0	7.0	1.37/1.37

FFE: Fast Field Echo, FSE: Fast Spin Echo, ^Pixel dimensions of registered images used for analysis

The recumbent MRIs were taken using a Philips 3 Tesla Ingenia. The scans were captured with the participant lying supine (Figure 2-1a) and for two breathing conditions: full inspiration and tidal expiration. The participants were asked to hold their breath in the required condition for the duration of the scan (approximately 25 seconds). Tidal expiration, as opposed to full expiration, was requested to minimise discomfort. For similar reasons, deep diaphragmatic inspiration, rather than maximal inspiration was requested. Two or three scan blocks were taken to capture the whole thoraco-abdominal region and registered together using the inbuilt Philips software. Three scan blocks were taken for the majority of participants, capturing the region from just above the spinous process (SP) of C7 to the mid-thigh. For participants who did not consent to having their pelvic region scanned, two blocks were used, covering the region from just above the C7 SP to the just below the sacroiliac joint. There was no information required for the current study which could not be obtained from the two most superior scan blocks.

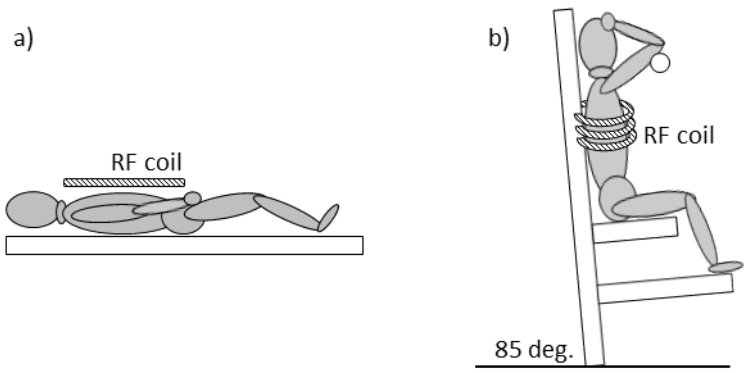

Figure 2-1 Participant and radiofrequency (RF) coil positions during (left) recumbent supine MRI scans and (right) upright MRI scans

A Fonar UPRIGHT® Multi-position MRI machine was used to collect the upright scans with the table set to its most vertical position (i.e. reclined 5° from the vertical). The upright scans were of considerable duration (approximately 8 minutes for each block), thus the participant was seated to reduce discomfort and movement (Figure 2-1b). The long scan duration precluded breath-holding techniques. Rather, the participants were instructed to breathe as shallowly as was comfortably possible in the vicinity of tidal expiration for the duration of the scan. It is inferred the shallow tidal breathing is of most similarity to the tidal expiration breathing condition of the recumbent scans.

The upright scans were taken in two blocks: capturing from just above the C7 spinous process to just below the lumbosacral junction. The upright MRI did not have the inbuilt software to register the two blocks together to form one image stack. Thus, image registration was completed using the semi-automatic 'Affine Registration' function in AMIRA (version 5.4.5, FEI, France) with block overlap and fiduciary markers on the skin surface used to align the scan blocks. The radiofrequency (RF) coil wrapped around the torso, requiring the participants to rest their arms on a superiorly-positioned support bar (Figure 2-1b). The coverage of the RF coil for the upright scans was not sufficient to cover the whole torso and thus required re-positioning between scans. Participants' posture was monitored during re-positioning and the potential for positional changes between scan blocks minimised. The upright scans were taken approximately 1.5 hours following the recumbent scans. Participants were asked to be well hydrated and to eat a light meal at least an hour before the first scanning session, with small snacks permitted between scanning sessions.

2.4. Image digitising

A combination of two medical image visualisation and analysis tools was used to quantify the positions of the anatomical points. Both AMIRA (version 5.4.5, FEI, France) and ImageJ (Version 1.46, NIH, USA) allowed for image projections in the orthogonal planes. Locating the precise locations of organ boundaries was achieved by harnessing the relative advantage of each program's visualisation and measurement tools. Locations were identified in AMIRA, and subsequently digitised in ImageJ. Points were digitised in the coronal plane with a resolution as determined by the scan pixel dimensions (Table 2-1). The resolution in the anteroposterior direction corresponded to the spacing between the scan slices (Table 2-1). The intra- and inter-rater reliability of the point digitisation was assessed (Appendix A).

Anatomical structures were identified for inclusion in the current analysis based on the stated coverage requirements in the literature. Thus, the organ boundaries of the heart, greater vessels, lungs, liver, spleen, kidneys and spine were identified (4-6). The X-coordinates of the lateral boundaries of each organ provide the data required for the analysis of armour width, and the Y-coordinates of the inferior boundaries provide the data required for the analysis of armour length. The Y-coordinates of the superior boundaries of the aortic arch and lungs were also used to analyse the coverage required at the top of the armour.

The most lateral boundaries of the pulmonary arteries (i.e. where they bifurcated) and venae cavae could not be identified precisely on the lower resolution upright scans, thus no upright data is provided for these points. The pulmonary vein bifurcations could not be identified precisely on either the recumbent or upright scans and were also excluded. All of these locations are closer to the mid-sagittal plane than the left cardiac border and thus were not deemed important for evaluating the dimensions of armour worn symmetrically around this plane. Not all participants consented to a scan of the pelvic region, thus the intestines were also excluded from the study as the inferior boundary was not captured for all participants.

To define the inferior boundaries of the thoracic and lumbar sections of the spinal cord, two points on the spine were utilised: the centre of the intervertebral discs (IVDs) T12-L1 and L5-S1. Only the superior and lateral boundaries of the lungs were digitised as the most inferior portions of the lungs are typically very narrow slivers of tissue on the rib cage which could not be identified consistently, especially on the upright scans. The point of the most superior concavity on the diaphragmatic surface of each lung was considered as the most functionally relevant point representing the inferior boundary of the majority of the lung tissue mass. The inferior points of the left and right lungs were estimated using the most superior boundaries of the spleen and liver respectively. These points offer conservative estimates of the highest concavity points of the lungs, due to the intermediate presence of the diaphragm. Twenty-seven anatomical points were used in the current coverage analysis (Table 2-2). The definitions for essential and desirable coverage identified by Breeze et al. (6) have been adopted for the purposes of hard and soft armour coverage analysis.

Table 2-2 Definitions of the anatomical points included for analysis, their classification as either essential (E) or desirable (D), and whether or not they were discernible on the upright scans.

#	Point Name	Point description	E/D	Upright
X-coordinates for the analysis of body armour width				
1	Left Cardiac	The most lateral point on the left cardiac border	E	Yes
2	Right Cardiac	The most lateral point on the right cardiac border	E	Yes
3	Left Pulmonary Artery	The bifurcation point of the left pulmonary artery	E	No
4	Right Pulmonary Artery	The bifurcation point of the right pulmonary artery	E	No
5	Lateral SVC	The right-most border of the SVC at the height that the brachiocephalic veins merge	E	No
6	Lateral Spleen (left)	The left-most boundary of the spleen	E	Yes
7	Lateral Liver (right)	The right-most boundary of the liver	E	Yes
8	Lateral Left Lung (SN)	The most lateral point of the left lung at the height of the SN	D	Yes
9	Lateral Left Lung	The most lateral point of the left lung	D	Yes
10	Lateral Right Lung (SN)	The most lateral point of the right lung at the height of the SN	D	Yes
11	Lateral Right Lung	The most lateral point of the right lung	D	Yes
12	Lateral Left Kidney	The left-most boundary of the left Kidney	D	Yes
13	Lateral Right Kidney	The right-most boundary of the right Kidney	D	Yes
Y-coordinates for the analysis of body armour length				
14	Superior Aorta	The most superior point of the aortic arch	E	Yes
15	Inferior Heart	The most inferior point of the heart	E	Yes
16	Inferior Aorta	The bifurcation point of the abdominal aorta into the iliac arteries	E	Yes
17	Inferior Vena Cava	The point of union of the common iliac veins	E	No
18	Inferior Spleen	The most inferior point of the spleen	E	Yes
19	Inferior Liver	The most inferior point of the liver	E	Yes
20	Superior Left Lung	The most superior point of left lung	D	Yes
21	Inferior Left Lung	The most superior point of the spleen representing the point of the highest concavity of the base of the left lung	D	Yes
22	Superior Right Lung	The most superior point of right lung	D	Yes
23	Inferior Right Lung	The most superior point of the liver representing the point of the highest concavity of the base of the right lung	D	Yes
24	Inferior Left Kidney	The most inferior point of the left kidney	D	Yes
25	Inferior Right Kidney	The most inferior point of the right kidney	D	Yes
26	Inferior Thoracic Spinal Cord	The approximate centre of the intervertebral disc T12-L1	D	Yes
27	Inferior Lumbar Spine Cord	The approximate centre of the intervertebral disc L5-S1	D	Yes

The data points in Table 2-2 represent the boundaries of organs and structures identified in the literature as important for body armour coverage. However, there are a number of structures for which data has been collected which has not been included in the current

analysis, including the pancreas and internal structures of organs such as the renal sinus of the kidneys. A large database of anatomical structure boundaries in each of the scan conditions is provided in Appendix B, Appendix C and Appendix D. Included in the database are additional points further describing the geometry of the heart, referred to as the atrial and ventricular bulges. These points describe the most superior-lateral regions of the left atrium and ventricle. This data is important as the armour front panel/plate is generally cut-away diagonally at the shoulder to allow for less hindered shoulder movement. Further defining the cardiac geometry allows the coverage implications of these cut-aways to be investigated.

2.5. Transforming coordinates to the Body Coordinate System

The global coordinate system of the scanner bed was transformed into a relevant body coordinate system (BCS, Figure 2-2) to compare and collate points for different participants. The SN was chosen as the origin of the BCS as it is an easily identifiable external anthropometric landmark that is often used as a reference point for positioning the top edge of hard body armour. Furthermore, the SN is in the mid-sagittal plane of the body and body armour is generally worn centred around this plane. The X- and Y-coordinates of the SN were defined separately. The X-component was defined as the middle of the superior aspect of the manubrium (i.e. the anatomical SN representing the body midline). The Y-component was defined as the superior-inferior midpoint of the fiduciary marker, which was positioned over the palpable SN, as defined in the AWAS (13, 14). Review of the MRIs indicated that the height of the anatomical SN is often more superior than the palpable SN. This is because the most superior point on the manubrium is sometimes too posterior (i.e. too deep) to be readily identified by palpation. Using the palpable SN for calculating the Y-coordinate of SN ensures that all results remain relevant for the practical application that motivated this research, that is, the fitting and positioning of body armour.

Figure 2-2 The body coordinate system with the origin at the SN (fiduciary marker shown) and the positive z-axis directed posteriorly.

Initially, a linear translation of the points moved the origin to the SN. Secondly, a rotational transformation of the points was performed about the Z-axis (anterior-posterior axis) to correct for any rotation in the participant's orientation about this axis on the MRI bed. The mid-sagittal line of the body (Y-axis) was taken to be the straight line from the SN to the middle of the pubic symphysis, the angle of which, relative to the long axis of the MRI bed, determined the angular correction required in the rotational transformation about the Z-axis. For upright scans, when the pubic symphysis was not in the field of view, the most inferior distinguishable point on the linear alba was used to define the body midline. The same approach was used for the recumbent scans for participants who did not consent to a pelvic scan.

2.6. Data analysis

2.6.1. Breathing and postural conditions statistical analysis

Data sets for each condition were assessed for normality using Shapiro-Wilk tests at $\alpha = 0.05$. Two-tailed Wilcoxon signed rank tests were used to identify significant effects of breathing and postural changes to organ positions. The Benjamini and Yekutieli false discovery rate (FDR) controlling procedure was adopted at $q = 0.05$ due to the large number of Wilcoxon signed rank tests (73 tests) (15). Cohen's d was also calculated where, if $d \geq 0.8$, the effect size was deemed large. Statistics were calculated using SPSS (v21) and MS Excel (2010).

2.6.2. Body armour coverage analysis

For the exemplar body armour coverage analysis, it was assumed that the wearer is in an upright position. Hence, only the upright data (n = 14) has been used for this purpose. Body armour is available in a range of sizes and dimensions. In the current analysis, exemplar body armour coverage analysis was conducted using body armour dimensions from the literature. Two sets of common dimensions of hard armour plates are defined by the NIJ, designated herein as small and large (16). The small plate is defined as 8 x 10 inches (203 x 254 mm) and the large plate as 10 x 12 inches (254 x 305 mm). These plate sizes can be assessed against the locations (both X- and Y-coordinates) of the essential anatomical structures to determine the perpendicular coverage which would be afforded to the scanned cohort by the small and large hard plates.

The upright data sets for each anatomical structure can be analysed in order to calculate the proportion of a population who would be covered by body armour of given dimensions. The data distributions for each anatomical structure were assessed for normality using the Shapiro-Wilk test at $\alpha = 0.05$. For data sets with a significance level greater than 0.05, it is reasonable to model the data as a normal distribution. The mean and SD were calculated for each dataset and used to compute cumulative normal probability distribution functions for each data set. These distributions were assumed to represent the male Australian Army population.

3. Results

3.1. Anthropometric measures

The anthropometry of the participants reflected reasonably well the variation within the AWAS population (13) (Table 3-1 and Figure 3-1). The mean anthropometric measurements of the participants fell within one standard deviation of the male AWAS mean values. The chest breadth measurements of the MRI scanned cohort of 23 participants ranged from the 2nd to the 82nd percentile of the male AWAS population; that of the upright subset of 14 participants ranged from the 4th to 78th percentile. The front length measurements of the MRI scanned cohort (and the upright subset) range from the 2nd to the 98th percentile.

Table 3-1 MRI cohort demographic and anthropometric descriptive statistics: mean (SD)

	Total cohort (n=23)	*Upright subset (n=14)*	*AWAS (n=1861)*
Age (years)	29.3 (6.5)	29.6 (4.7)	24.9 (4.7)
Mass (kg)	84.5 (10.4)	86.0 (11.9)	82.7 (12.2)
Stature (mm)	1821.7 (71.7)	1836.1 (48.2)	1785.0 (68.3)
Sitting Height (mm)	958.7 (32.5)	953.2 (35.1)	936.0 (34.1)
Front Length (mm)	365.9 (27.6)	365.0 (28.3)	362.0 (24.0)
Chest Breadth (mm)	299.2 (27.6)	298.6 (17.8)	305.0 (25.7)*

* n=1860

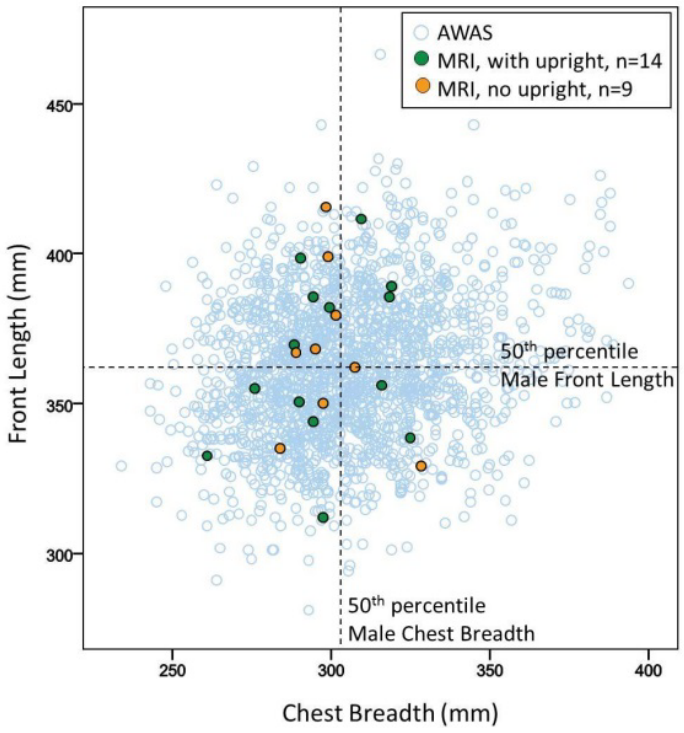

Figure 3-1 Scatter plot of chest breadth versus front length for the AWAS males dataset (n=1860) and the MRI dataset (n=23), the latter categorised based on the availability of upright data for each participant.

3.2. Anatomical variability between breathing/postural conditions

Descriptive statistics and Shapiro-Wilk significance values for the locations of the anatomical points of interest are shown for the 'expiration' (supine, tidal expiration, Table 3-2), 'inspiration' (supine, deep diaphragmatic inspiration, Table 3-2) and 'upright' (seated, shallow tidal breathing, Table 3-3) scan conditions. Most datasets did not violate the assumption of normality as shown by Shapiro-Wilk significance values greater than 0.05.

The data presented represents the boundaries of organs and structures identified in the literature as important for body armour coverage. However, there are a number of other structures for which data has been collected, including the pancreas and internal structures of organs such as the hilum of the spleen and renal sinus of the kidneys. A large database all points digitised in each of the scan conditions is provided in Appendix B, Appendix C and Appendix D. These points also include the Z-coordinates which describe the anteroposterior locations of the structures.

Table 3-2 Anatomical locations and Shapiro-Wilk (SW) significance for the supine conditions

#		Total MRI cohort (n=23) Mean	SD	Min.	Max.	SW sig.	Upright subset of total MRI cohort (n=14) Mean	SD	Min.	Max.	SW sig.
Expiration recumbent condition											
X-coordinates											
1	Left cardiac border	102.6	9.7	89.7	124.9	0.209	103.5	11.5	89.7	124.9	0.313
2	Right cardiac border	-44.5	6.5	-59.0	-29.8	0.971	-43.6	7.5	-59.0	-29.8	0.965
3	Left Pulmonary Artery	53.7	3.7	47.2	63.6	0.535	55.2	3.7	49.6	63.6	0.475
4	Right Pulmonary Artery	-25.4	5.1	-34.3	-14.0	0.425	-24.1	5.6	-34.3	-14.0	0.807
5	Lateral SVC	-36.4	5.6	-45.7	-27.4	0.237	-35.1	5.8	-45.7	-27.4	0.211
6	Lateral Spleen (left)	139.3	9.3	116.3	155.6	0.089	139.9	10.8	116.3	155.6	0.097
7	Lateral Liver (right)	-138.9	7.4	-152.9	-125.1	0.809	-140.2	8.1	-152.9	-125.1	0.413
8	Lateral Left Lung (SN)	96.4	10.9	80.1	115.5	0.233	95.3	11.4	80.1	115.5	0.357
9	Lateral Left Lung	136.8	7.6	115.5	150.2	0.027‡	136.4	9.4	115.5	150.2	0.189
10	Lateral Right Lung (SN)	-94.7	9.6	-116.8	-80.1	0.219	-92.6	8.5	-106.7	-80.1	0.385
11	Lateral Right Lung	-133.3	6.4	-145.1	-120.0	0.818	-133.2	7.2	-143.5	-120.0	0.191
12	Lateral Left Kidney	104.6	7.6	87.2	123.0	0.136	105.6	8.8	87.2	123.0	0.137
13	Lateral Right Kidney	-102.5	7.2	-115.8	-89.2	0.788	-103.3	7.9	-115.8	-89.2	0.867
Y-coordinates											
14	Superior Heart/Aorta	6.3	7.3	-11.6	22.3	0.847	7.7	7.2	-5.6	22.3	0.994
15	Inferior Cardiac	190.1	14.9	159.1	214.6	0.622	187.8	16.4	159.1	213.3	0.562
16	Inferior Aorta	379.9	19.8	328.7	428.7	0.168	382.2	22.0	328.7	428.7	0.167
17	IVC	412.0	18.9	364.1	460.3	0.271	414.3	21.6	364.1	460.3	0.337
18	Inferior Spleen	262.5	23.8	215.0	310.4	0.893	266.2	26.3	215.0	310.4	0.930
19	Inferior Liver	319.0	23.7	270.2	352.7	0.451	317.2	27.0	270.2	352.7	0.390
20	Lung-Most superior left	-38.3	10.2	-63.9	-15.4	0.546	-35.0	9.8	-56.7	-15.4	0.898
21	Inferior Left Lung	155.5	14.0	127.4	186.5	0.998	155.8	16.7	127.4	186.5	1.000
22	Superior Right Lung	-36.9	9.8	-64.8	-17.0	0.156	-33.0	7.4	-45.4	-17.0	0.468
23	Inferior Right Lung	134.4	21.5	88.9	178.1	0.960	131.3	24.7	88.9	178.1	0.604
24	Inferior Left Kidney	321.4	19.0	292.7	370.7	0.534	324.9	19.8	292.7	370.7	0.736
25	Inferior Right Kidney	331.3	21.6	298.8	387.0	0.279	329.9	25.1	298.8	387.0	0.239
26	Inferior Thoracic Spine	247.4	20.1	212.2	286.1	0.806	250.4	18.1	222.3	286.1	0.814
Inspiration recumbent condition											
X-coordinates											
1	Left cardiac border	92.4	8.5	80.6	115.4	0.106	92.8	9.6	80.6	115.4	0.158
2	Right cardiac border	-44.1	6.9	-59.1	-26.9	0.928	-43.2	8.2	-59.1	-26.9	0.993
3	Left Pulmonary Artery	51.2	5.2	44.4	61.8	0.142	52.5	5.3	44.8	61.8	0.500
4	Right Pulmonary Artery	-28.0	5.3	-39.5	-16.1	0.850	-28.4	6.2	-39.5	-16.1	0.938
5	Lateral SVC	-32.2	6.5	-44.2	-21.7	0.681	-30.9	7.2	-44.2	-21.7	0.471
6	Lateral Spleen (left)	142.0	9.0	118.1	162.3	0.393	143.1	10.8	118.1	162.3	0.737
7	Lateral Liver (right)	-142.6	7.7	-156.5	-127.8	0.453	-144.1	7.5	-156.5	-129.1	0.461
8	Lateral Left Lung (SN)	99.9	10.8	83.1	119.4	0.477	98.6	12.0	83.1	119.4	0.383
9	Lateral Left Lung *	144.1	9.7	114.8	158.6	0.008	143.2	11.6	114.8	158.6	0.097
10	Lateral Right Lung (SN)	-96.4	10.2	-118.1	-77.9	0.424	-94.1	9.5	-108.9	-77.9	0.548
11	Lateral Right Lung	-140.9	7.3	-152.1	-126.0	0.451	-140.2	8.1	-152.1	-126.0	0.818
12	Lateral Left Kidney	107.2	7.4	91.3	125.7	0.328	108.2	8.3	91.3	125.7	0.782
13	Lateral Right Kidney	-103.4	7.1	-114.8	-89.3	0.407	-104.0	7.5	-114.8	-89.3	0.312
Y-coordinates											
14	Superior Heart/Aorta	16.5	8.6	-3.7	31.9	0.934	18.7	7.0	8.5	31.9	0.575
15	Inferior Cardiac	208.3	15.6	173.5	236.5	0.785	207.0	16.3	173.5	235.6	0.213
16	Inferior Aorta	385.3	20.2	332.7	425.6	0.411	388.0	21.4	332.7	425.6	0.217
17	IVC	415.9	20.7	371.6	464.2	0.975	417.3	22.5	371.6	464.2	0.948
18	Inferior Spleen	291.5	27.8	237.9	330.2	0.187	293.9	29.2	237.9	330.2	0.392
19	Inferior Liver	353.1	29.5	291.5	408.6	0.976	352.9	32.1	291.5	397.8	0.661
20	Lung-Most superior left	-36.8	10.1	-62.2	-15.3	0.911	-32.8	9.2	-52.6	-15.3	0.972
21	Inferior Left Lung	187.0	18.8	139.2	220.4	0.191	185.9	18.4	139.2	217.7	0.193
22	Superior Right Lung	-36.0	10.5	-64.7	-16.2	0.115	-31.5	7.3	-43.7	-16.2	0.707
23	Inferior Right Lung	169.2	22.5	109.4	209.7	0.380	168.2	23.8	109.4	196.9	0.046‡
24	Inferior Left Kidney	344.1	22.4	305.5	382.4	0.354	347.0	20.8	305.5	382.4	0.590
25	Inferior Right Kidney	357.6	25.5	318.6	405.9	0.286	357.6	27.7	318.6	405.9	0.395
26	Inferior Thoracic Spine	250.6	21.1	212.2	287.4	0.807	254.3	18.3	223.1	287.4	0.944
27	Inferior Lumbar Spine	434.5	26.0	384.6	475.6	0.682	438.0	24.9	384.6	475.6	0.923
27	Inferior Lumbar Spine	431.0	24.5	380.6	473.4	0.888	433.7	23.9	380.6	473.4	0.899

‡ Shapiro-Wilk significance < 0.05; data violates assumption of normality

Table 3-3 Anatomical locations and Shapiro-Wilk (SW) significance for the upright condition

Upright		*Upright subset of total MRI cohort (n=14)*				
#		**Mean**	**SD**	**Min.**	**Max.**	**SW sig.**
X-coordinates						
1	Left cardiac border	95.1	10.5	77.4	111.7	0.863
2	Right cardiac border	-43.4	6.6	-54.8	-29.0	0.801
6	Lateral Spleen (left)	133.9	10.2	115.8	146.9	0.297
7	Lateral Liver (right)	-134.6	10.2	-147.2	-111.2	0.211
8	Lateral Left Lung (SN)	97.9	11.0	76.6	118.3	0.975
9	Lateral Left Lung	137.4	9.9	117.9	148.7	0.060
10	Lateral Right Lung (SN)	-94.4	10.7	-114.2	-80.7	0.145
11	Lateral Right Lung	-133.7	8.9	-151.0	-116.1	0.270
12	Lateral Left Kidney	106.4	7.2	92.4	118.0	0.529
13	Lateral Right Kidney ^	-98.1	10.6	-112.2	-76.8	0.245
Y-coordinates						
14	Superior Heart/Aorta	20.8	7.4	2.1	30.2	0.165
15	Inferior Cardiac	218.2	19.3	192.0	267.1	0.245
16	Inferior Aorta	380.0	26.5	323.3	440.9	0.468
18	Inferior Spleen	309.6	29.5	263.6	369.3	0.779
19	Inferior Liver	366.9	25.8	318.1	418.7	0.999
20	Lung-Most superior left	-37.4	8.0	-54.0	-24.6	0.938
21	Inferior Left Lung	184.9	22.8	156.1	232.1	0.337
22	Superior Right Lung	-34.9	7.9	-48.8	-19.0	0.997
23	Inferior Right Lung	171.4	23.3	138.6	222.6	0.341
24	Inferior Left Kidney	353.6	29.5	316.8	430.8	0.105
25	Inferior Right Kidney ^	360.8	44.9	288.1	452.9	0.649
26	Inferior Thoracic Spine	244.2	18.5	204.0	269.0	0.508
27	Inferior Lumbar Spine ^	429.1	25.5	385.4	462.3	0.491

^ n=13 due to inability to confidently locate these points on the scans for one participant (same participant for points 13 and 25 and different participant for point 27)

Variations in the boundaries of thoraco-abdominal organs due to breathing and postural conditions were analysed with the X- and Y- coordinates separately, representing the lateral and superior/inferior boundaries of organs respectively (Figure 3-2, Table 3-4). Organ boundary movement has been quantified as the difference between the expiration and inspiration conditions (n = 23), the expiration and upright conditions (n = 14), and the inspiration and upright conditions (n = 14). Adopting the FDR controlling procedure at $q = 0.05$, the Wilcoxon signed rank test significance level was set at $p \leq 0.005$.

The inspiration condition generally resulted in the most lateral organ boundaries for the spleen, liver, kidneys and lungs (as denoted by positive mean differences for structures positioned to the left of the mid-sagittal plane and negative mean differences for structures to the right of the mid-sagittal plane). Conversely, the left cardiac border was most laterally positioned during the expiration condition. The mean change in the position of the right cardiac border between conditions was small and not significant. The majority of mediolateral movement of organs due to changes in the breathing conditions was significant, however the effect sizes were not large with the exception of the lateral lung boundaries and the left cardiac border, which was positioned an average of 10.2 mm more laterally during expiration. The majority of mediolateral movement between the expiration and upright conditions was not significant.

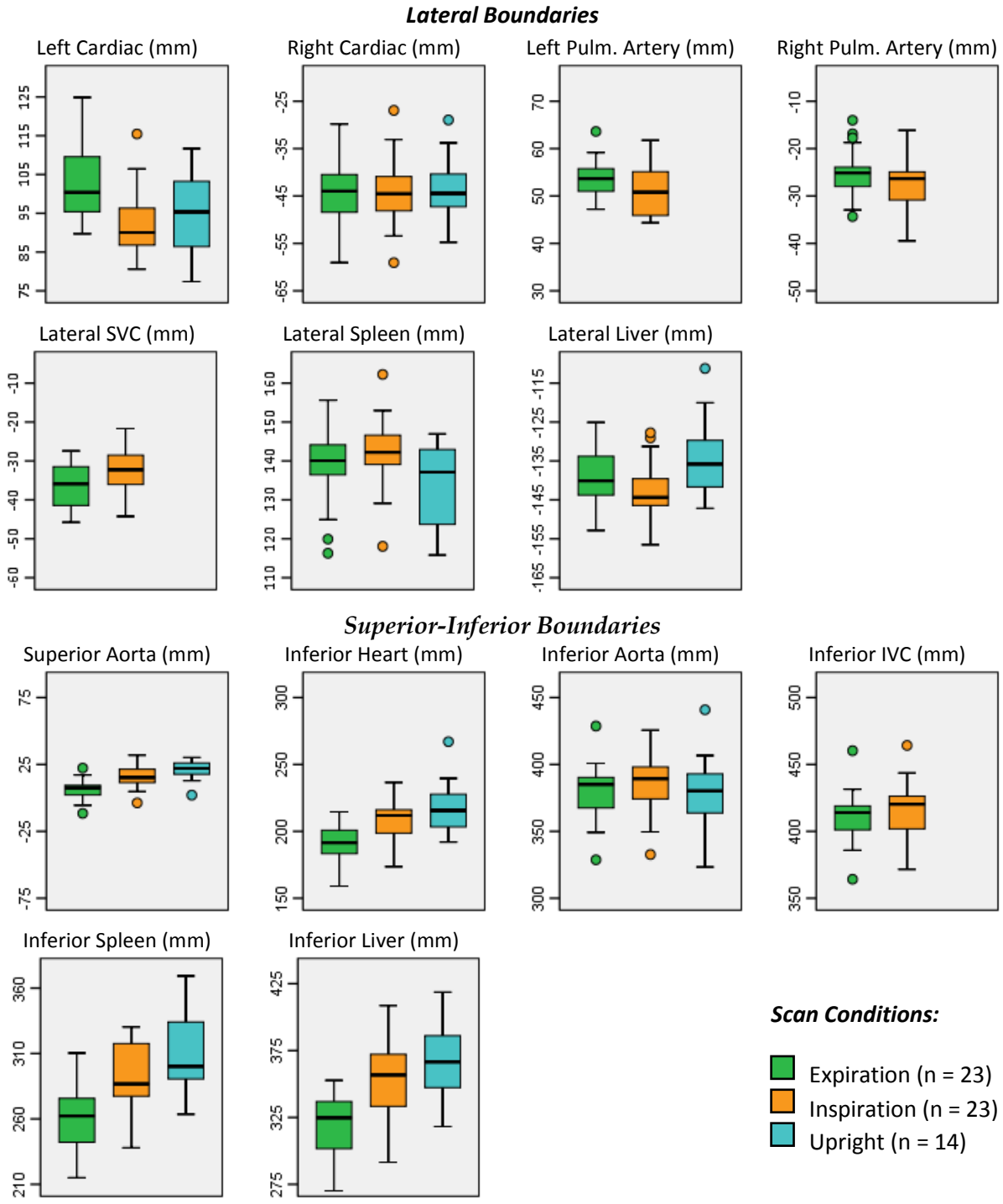

Figure 3-2 Five number summaries (minimum, first quartile, median, third quartile and maximum) for the varying locations of the essential structures under each breathing and postural condition. Values represented as a horizontal distance from the body midline for the lateral boundaries of structures; and as a distance from the SN for the superior-inferior boundaries of structures. All values in mm. Outliers greater than 1.5 box lengths from the lower or upper hinge of the box represented by dots.

Table 3-4 Movement of the anatomical structure boundary positions under different breathing and postural conditions. Descriptive statistics, Wilcoxon signed rank (WSR) tests significance level and effect sizes are shown.

#	Organ Boundary or Anatomical Structure	Expiration to Inspiration (n = 23)					Expiration to Upright (n = 14)					Inspiration to Upright (n = 14)				
		Mean (mm)	SD	Range (mm)	*WSR p*-value	Cohen's *d*	Mean (mm)	SD	Range (mm)	*WSR p*-value	Cohen's *d*	Mean (mm)	SD	Range (mm)	*WSR p*-value	Cohen's *d*
X-coordinates (lateral boundaries)																
1	Left Cardiac	-10.2	7.7	-27.5 to 2.2	<0.001*	-1.12†	-8.4	10.9	-32.8 to 4.5	0.013	-0.77	2.3	9.0	-8.1 to 21.7	0.594	0.23
2	Right Cardiac	0.5	3.1	-5.4 to 4.9	0.429	0.07	0.2	7.2	-13.5 to 13.0	0.875	0.03	-0.2	7.7	-16.4 to 11.6	0.730	-0.03
3	Left Pulmonary Artery	-2.5	4.4	-11.7 to 6.3	0.012	-0.55										
4	Right Pulmonary Artery	-2.6	6.1	-22.6 to 2.5	0.128	-0.50										
5	Lateral SVC	4.2	2.7	-0.4 to 9.1	<0.001*	0.70										
6	Lateral Spleen (left)	2.6	3.2	-2.9 to 9.5	0.001*	0.29	-6.0	6.9	-21.2 to 4.0	0.005*	-0.57	-9.2	7.3	-26.9 to 2.2	0.001*	-0.88†
7	Lateral Liver (right)	-3.7	2.7	-10.0 to 1.5	<0.001*	-0.49	5.7	8.6	-9.0 to 18.6	0.041	0.61	9.5	7.9	-2.8 to 21.2	0.003*	1.06†
8	Lateral Left Lung (SN)	3.5	2.3	0.4 to 8.3	<0.001*	0.32	2.6	8.7	-10.2 to 18.4	0.397	0.23	-0.8	8.6	-13.7 to 11.9	0.826	-0.07
9	Left lung	7.3	4.7	-0.8 to 18.2	<0.001*	0.84†	0.9	7.1	-8.7 to 18.1	0.510	0.10	-5.9	8.3	-20.9 to 10.3	0.035	-0.55
10	Lateral Right Lung (SN)	-1.7	2.1	-5.7 to 2.2	0.002*	-0.17	-1.7	9.7	-26.6 to 8.4	0.826	-0.18	-0.2	10.4	-28.7 to 9.8	0.594	-0.02
11	Right lung	-7.6	4.2	-15.9 to 0.5	<0.001*	-1.12†	-0.5	7.1	-11.5 to 8.8	0.730	-0.06	6.5	7.8	-3.6 to 21.0	0.016	0.77
12	Left Kidney Lateral	2.6	2.9	-2.5 to 10.2	<0.001*	0.35	0.8	7.1	-11.5 to 12.6	0.730	0.10	-1.8	6.9	-14.2 to 11.9	0.363	-0.23
13	Right Kidney Lateral ‡	-0.9	2.2	-7.0 to 2.2	0.101	-0.12	5.6	9.2	-9.0 to 20.2	0.064	0.56	5.8	8.5	-8.5 to 19.6	0.039	0.64
Y-coordinates (superior/inferior boundaries)																
14	Superior Heart/Aorta	10.1	4.8	1.3 to 18.4	<0.001*	1.27†	13.1	10.0	-10.6 to 28.0	0.003*	1.80†	2.1	9.0	-11.9 to 15.0	0.433	0.29
15	Inferior Cardiac	18.2	5.4	9.9 to 29.5	<0.001*	1.20†	30.4	12.6	6.3 to 53.8	0.001*	1.69†	11.2	9.9	-4.0 to 31.5	0.004*	0.62
16	Inferior Aorta	5.3	4.0	-3.1 to 13.9	<0.001*	0.27	-2.2	12.4	-27.3 to 12.7	0.683	-0.09	-8.0	11.9	-32.6 to 15.2	0.048	-0.33
17	IVC	3.8	7.5	-20.5 to 14.1	0.006	0.19										
18	Inferior Spleen	29.0	14.2	8.3 to 64.2	<0.001*	1.12†	43.4	19.6	3.4 to 78.3	0.001*	1.55†	15.7	23.1	-24.6 to 63.2	0.026	0.53
19	Inferior Liver	34.1	14.2	14.4 to 60.9	<0.001*	1.27†	49.7	22.9	-4.9 to 74.4	0.001*	1.88†	14.0	27.2	-28.7 to 53.7	0.084	0.48
20	Superior Left Lung	1.5	1.9	-2.3 to 6.6	0.001*	0.15	-2.4	10.0	-22.8 to 17.5	0.363	-0.27	-4.5	8.8	-22.9 to 13.4	0.084	-0.53
21	Inferior Left Lung	31.5	14.3	8.5 to 65.1	<0.001*	1.90†	29.1	20.7	-12.3 to 63.5	0.003*	1.45†	-1.0	20.9	-40.9 to 37.9	0.638	-0.05
22	Superior Right Lung	1.0	2.1	-4.0 to 6.2	0.021	0.10	-1.9	7.8	-18.6 to 10.8	0.510	-0.25	-3.4	7.5	-19.4 to 9.4	0.124	-0.45
23	Inferior Right Lung	34.8	15.4	7.6 to 67.5	<0.001*	1.58†	40.1	25.1	-20.5 to 74.4	0.002*	1.67†	3.2	24.1	-39.6 to 48.1	0.683	0.14
24	Inferior Left Kidney	22.7	11.3	6.6 to 48.5	<0.001*	1.09†	28.7	20.7	-17.7 to 60.1	0.002*	1.14†	6.6	22.6	-35.3 to 48.4	0.300	0.26
25	Inferior Right Kidney ‡	26.3	11.9	10.0 to 48.5	<0.001*	1.11†	30.3	26.0	-33.5 to 65.9	0.005*	0.85†	2.1	25.3	-43.7 to 47.0	0.807	0.09
26	Inferior Thoracic Spine	3.2	3.0	-0.6 to 9.7	<0.001*	0.15	-6.2	11.2	-27.8 to 7.6	0.096	-0.34	-10.1	9.3	-28.7 to 1.3	0.002*	-0.55
27	Inferior Lumbar Spine ‡	3.5	3.6	-3.1 to 10.5	<0.001*	0.14	-3.1	11.3	-21.2 to 12.1	0.422	-0.19	-7.2	9.4	-24.7 to 3.8	0.039	-0.35

* Wilcoxon signed rank test significant at $p \leq 0.005$

† Large effect size, $|d| > 0.8$

‡ n = 13 for upright data

The thoraco-abdominal organs were generally positioned more caudally during the inspiration and upright conditions (as denoted by positive mean differences). Statistical significance and large effect sizes were observed for caudal movement of the superior aorta and the inferior boundaries of the heart, lungs, liver, spleen and kidneys for the inspiration and upright conditions compared with expiration. Although the mean differences in inferior cardiac border and inferior thoracic spine were significant between the inspiration and upright conditions, the associated effect sizes were not large. There were no other significant changes or large effect sizes for any of the Y-coordinates between the inspiration and upright conditions.

3.3. Exemplar body armour coverage analysis

The X- and Y-coordinates of the anatomical boundary dataset can be used to assess the dimensions of existing or proposed body armour systems against perpendicular threats. The NIJ-defined common hard plate sizes were assessed against the upright anatomical points for which body armour coverage is deemed essential (6) and where plates were assumed to be worn at the SN (Figure 3-3).

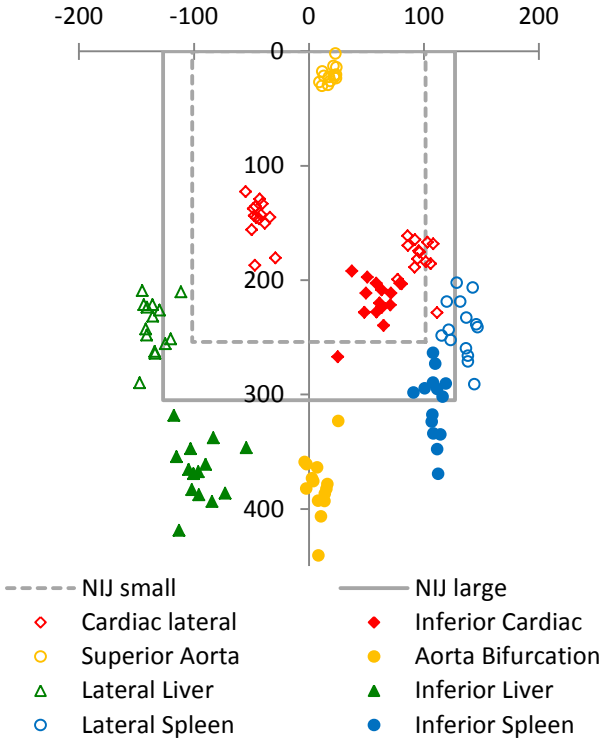

Figure 3-3 *Coverage of essential anatomical structures in the upright posture (n = 14) provided by the NIJ common plate sizes worn at the SN (0, 0). The small plate is defined as 8 x 10 inches (203 x 254 mm) and the large plate is 10 x 12 inches (254 x 305 mm). Axes are in mm.*

Perpendicular coverage would be provided to the superior point of the aorta for all upright participants. The small plate would cover the heart for the majority of the cohort, however, the inferior cardiac border of one participant and the left cardiac border of five participants would be exposed by this plate. The small plate does not provide perpendicular coverage to the boundaries of the spleen, liver or the inferior boundary of the abdominal aorta of any participants. The large plate provides coverage to all cardiac boundaries for the entire cohort and coverage to the inferior boundaries of the spleen for eight participants. The lateral boundaries of the spleen and liver are covered by the large plate for a minority of participants (three and four participants, respectively). However, the inferior boundary of the liver and the abdominal aorta are not afforded coverage for any members of the scanned cohort.

Thus, both the small and large NIJ hard plate dimensions are too small if the primary objective is perpendicular coverage of the anatomical structures considered essential by Breeze et al (6). Although the large plate provides coverage to the cardiac borders of all participants, this analysis indicates that sufficient perpendicular coverage of the liver, spleen and abdominal aorta would not be afforded to a significant proportion of the scanned cohort by a plate of this size. The NIJ small and large plates were defined as rectangular, however, the majority of front plates have the top corners cut away to allow for less hindered shoulder movement. As Figure 3-3 demonstrates, this can likely be achieved with minimal loss of perpendicular coverage of the essential structures.

3.4. Coverage probability distribution functions

Cumulative distribution functions can be used to estimate the proportion of the Australian male population who would be afforded perpendicular coverage by body armour of given dimensions. None of the upright datasets violated the assumption of normality, based on the Shapiro-Wilk test; thus, the parametrised cumulative probability curves are shown for all upright datasets (Figure 3-4). The distribution curves can be used to estimate the percentage of the male Australian Army population that would be afforded essential or desirable coverage (6), for each organ boundary, in the upright position, for a given armour width or length. For example, a hard plate of length 350 mm would cover the whole length of the heart for 100% of the Australian Army population, while 91%, 26% and 13% would be afforded coverage of the whole lengths of the spleen, liver and abdominal aorta respectively.

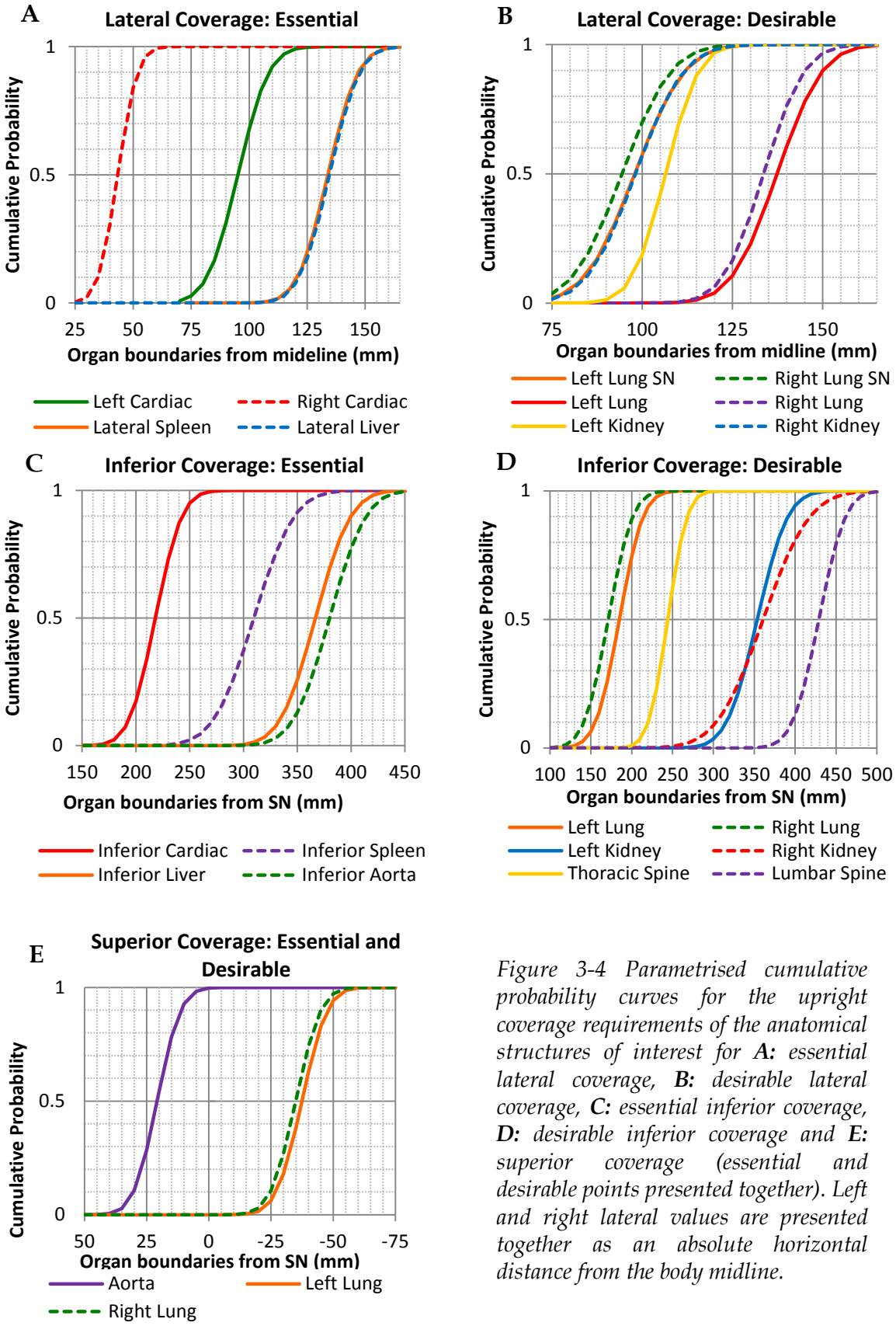

*Figure 3-4 Parametrised cumulative probability curves for the upright coverage requirements of the anatomical structures of interest for **A:** essential lateral coverage, **B:** desirable lateral coverage, **C:** essential inferior coverage, **D:** desirable inferior coverage and **E:** superior coverage (essential and desirable points presented together). Left and right lateral values are presented together as an absolute horizontal distance from the body midline.*

4. Discussion

This is the first study to quantify the effect of breathing and posture on the positions of various internal thoraco-abdominal organ boundaries of a cohort. Both inspiration and orienting upright caused significant caudal shifting of the organs relative to the expiration condition. The results of this study can be used to better understand the movement of internal organs due to breathing and postural changes and aid in the assessment and design of body armour.

4.1. Implications of breathing and postural conditions for body armour analyses

The boundaries of anatomical structures for which coverage is required vary significantly due to breathing and postural changes. Relative to supine expiration, supine inspiration results in more vulnerable inferior organ boundaries for the majority of analysed structures and more vulnerable lateral organ boundaries for the lungs, spleen and liver. The latter is likely due to the expansion of the chest width during inspiration and the close relationships between the chest wall and the lateral surfaces of the lungs, liver and spleen. However, the expiration condition should also be considered when determining body armour width requirements and the positioning of the top edge of worn body armour. The left cardiac border was positioned 10.2 ± 7.7 mm more laterally during expiration than inspiration and the superior boundary of the aorta was 10.1 ± 4.8 mm more cranial, increasing the potential for exposure at the top of worn armour.

The average inferior boundaries of the heart, spleen, liver, lungs and kidneys all shifted caudally from the supine tidal expiration condition to the upright posture. The greatest movement was observed at the inferior boundaries of the liver and spleen, shifting caudally 49.7 ± 22.9 mm and 43.4 ± 19.6 mm respectively, from the expiration to upright conditions. It is assumed that the upright shallow tidal breathing condition is similar to the supine tidal expiration condition, in terms of lung volume, and therefore, the majority of organ movement is a result of gravitational force on the organs. This assumption is supported by the similar lateral lung boundaries between expiration and upright conditions, suggesting a similar lung capacity during the scans. Regardless, consideration should be given to the limited respiratory control between the supine and upright conditions when interpreting the upright results. Although the inferior boundaries of the heart, liver, spleen and kidneys were all generally positioned more caudally during the upright condition than the inspiration condition, the only significant difference was observed at the inferior cardiac border.

The use of the upright data for coverage analysis is important as it represents a frequent posture adopted by combatants and generally results in more vulnerable inferior organ boundaries. However, the use of this data it is not definitively the most conservative approach to coverage. Although the upright data has been used for exemplar analysis herein, sufficient data has been provided should future researchers wish to conduct analysis using the most conservative available data for each anatomical point of interest.

Notwithstanding, it is unlikely that the absolute worst case or most vulnerable position for each organ has been captured in the three scan conditions included in this study. Furthermore, the supine data herein should not be interpreted as the same as in the prone position; it has previously been reported that when prone, the heart, liver, spleen and kidneys all shift caudally from their positions while supine (17).

4.2. Comparisons with existing data

A number of studies have investigated respiration-induced organ motion for radiotherapy applications (18-21); however, most have studied the movement of the centre of the organ (18-20), involved cancer patients (19-21) and adopted 'normal breathing' techniques (18-20). Thus, the results of these studies are not directly comparable with the current study, where deep inspiration and tidal expiration techniques were instructed to the healthy participants and the points of measurement were the organ boundaries. The average magnitudes of superior-inferior movement for the heart, liver, spleen and kidneys in this study were consistently greater than those observed in the literature for normal breathing (18-20). The use of the sternal notch as the reference point from which organ measurements were taken may have also contributed to the greater values observed for the superior-inferior movement of organs in this study compared to those in the literature. During inspiration the sternum, and thus the sternal notch, translate anteriorly and superiorly, as part of the mechanics of breathing (22), thus resulting in greater obtained values of inferior movement of organ boundaries than would be observed from the global reference frame of the scanner bed[1]. Regardless of any movement of the origin relative to the scanner bed, the sternal notch is the most relevant reference point for this study due to its importance when fitting and positioning body armour and the likelihood that an armour plate would move with the sternal notch during respiration.

There is limited data in the literature to compare the magnitudes of organ movement between supine and upright (~ 90° to the horizontal) conditions for more than a single participant. Beillas et al. (8) calculated the movement of the CoG of the liver, spleen and kidneys of nine participants (six males and three females) in different postural conditions. As in the current study, only small variations were seen in the lateral positions of the studied organs as a result of postural changes. Moving from supine to standing position (same table angle as the current study), the inferior movement of the CoG of the organs was calculated for the liver, spleen and kidneys with average values slightly, but consistently, less than those observed in the current study. Such small discrepancies are likely due to methodological differences in breathing conditions, reference frame and origin, inclusion of females and use of the organ CoG (8).

There is a dearth of comparable data in the literature on the mediolateral motion of the heart and greater vessels due to respiration. The mean value of left-to right movement of the heart centre of mass and the left anterior descending coronary artery during normal breathing have been reported as 2.1 ± 1.4 mm (20) and 2.58 ± 4.9 mm (21) respectively.

[1] In the current study, the SN was positioned on average 2.7 ± 2.7 mm more superiorly during inspiration than expiration (range: -1.3 to 8.8 mm).

Such values are substantially less than the movement of the left cardiac border observed herein, likely due to the more medial points of measurement in the previous studies.

The recumbent organ boundary data can be compared with the reported values of Breeze et al. (7). The left cardiac border mean position in the inspiration condition is very similar to that of Breeze et al., however the mean expiration value in the current study was much more lateral, falling between the reported 75th and 95th percentile values of Breeze et al. (7). The mean right cardiac border locations in the current study equated to approximately the 75th percentile value of Breeze et al. for both expiration and inspiration conditions.

The inferior organ boundary data of Breeze et al. is presented as various vertical distances between two anatomical structures rather than from the SN. As such, values for comparison have to be calculated from the reported data herein. The mean lengths of the aorta (from aortic arch to bifurcation) in the current study, for both inspiration and expiration conditions, are slightly greater than the 75th percentile values reported by Breeze et al. (7). There was a large difference between the two studies with regard to the length from the aortic arch to the inferior boundary of the liver; the mean values for the expiration and inspiration conditions in the current study equated to approximately the 95th, and the much greater than the 95th percentile of values reported by Breeze et al. respectively (7). The greater stature of the current cohort, the mean of which was approximately that of the 75th percentile of Breeze et al., may explain some of the observed differences in results. However, Breeze et al. found little correlation between stature and the lengths of essential medical coverage (7). The front length (or torso height) anthropometric data reported by Breeze et al. was collected from the CT scans of the cohort, with a 50th percentile value of 371 mm; considerably less than 392 mm, the MRI-derived mean front length of the current cohort. Consistent discrepancies have been found in anthropometric measures obtained using traditional methods and those from medical images (23). Thus, comparing the MRI-derived front length measurement of the current cohort (392 mm) is more appropriate than that derived using traditional anthropometric methods (366 mm).

4.3. Body armour coverage assessments

The upright MRI data has been used to evaluate body armour coverage when the wearer is in an upright posture. Exemplar coverage analysis using the NIJ-defined common hard plate dimensions suggests the hard plate dimensions should be larger to provide perpendicular coverage to the essential anatomical structures of the thorax and abdomen. Furthermore, due to potentially sub-optimal ballistic performance near the edges of armour, the effective area of coverage is less than the total area of the armour. However, the increased coverage provided by larger plates must be considered against the ergonomic and performance costs of increased plate dimensions and thus increased mass.

The only similar published body armour coverage analysis known to the authors is that provided by Breeze et al. (6), where the perpendicular coverage provided by the UK Osprey Mk4 hard plate was assessed using the commercially-available Zygote anatomical model. The plate was assessed to have provided perpendicular essential coverage to all the

required structures (excluding the abdominal aorta and IVC). However, the anatomy of the Zygote model is mostly based on a single male (approximately 50th percentile) in a supine condition (24); therefore it may not reflect the vulnerability of different populations or upright postures.

Parametrised distributions of the upright organ boundary data have been presented for future use in simple perpendicular coverage analyses of existing or proposed body armour dimensions. The organ boundary data enables researchers to estimate the proportion of the population whose anatomical structures would be wholly covered.

4.4. Limitations

The current study provides the largest available dataset of organ boundary values in varied breathing and postural conditions; however, the sample size is much smaller than that desired for population reference databases. Although the participants were all healthy males within the typical age ranges of military or police populations, the varying age and external anthropometry of the participants likely caused variations in the data. The width coverage analysis of the MRI cohort is likely to be overestimating the coverage that would be afforded to individuals of chest breadth greater than the 82nd percentile in AWAS, or 78th percentile in AWAS if using only the upright subset. Conversely, the front length measurements of the MRI scanned cohort (and the upright subset) range from the 2nd to the 98th percentile; indicating the cohort effectively captured the variability of the wider population.

This study was limited to males however the methods described herein have been adopted in a pilot study of three females, the data from which is published elsewhere (25). Future studies should include a sufficient number of females to quantify the coverage requirements of the entire female combat force.

The upright scans were taken approximately 1.5 hours following the recumbent scans; therefore it is possible that organ positions may have been altered due to ingestion or biological processes such as digestion and urination. Any organ movement due to these processes is assumed to be random rather than systematic.

The population data provided enables researchers to estimate the proportion of the population whose anatomical structures would be wholly covered. However, in the instance of partial organ coverage, it is not possible to determine the percentage of the organ volume which is afforded coverage. MRI segmentation methods would facilitate such analysis. However, segmentation methods are very time-consuming to conduct manually, and it is anticipated that the manual identification of the points of interest provides a more accurate method of data collection than semi-automated segmentation methods. Moreover, in the case of partial organ coverage, it is the authors' belief that knowledge of the coverage of the heavily vascularised regions of the organs is more important for body armour coverage considerations than the proportion of the organ covered. Thus, included in Appendix B, Appendix C and Appendix D is information on

the lateral and inferior boundaries of the hilum of the spleen, the renal sinus of the kidneys and the vasculature in the liver.

Vulnerability analysis herein has been limited to the coverage afforded against perpendicular assaults. The creation or refinement of anatomically accurate 3D human computational models will allow for the analysis of coverage and vulnerability against obliquely directed assaults, such as fragmentation threats originating from buried explosive devices.

Although the supine inspiration and upright (expiration) conditions provide more conservative values for the analysis of body armour length than the supine expiration condition, it is likely that an upright inspiration condition would result in further caudal movement of the inferior organ boundaries. However, the superior-inferior movement of the diaphragm during respiration in the supine position has been found to be significantly greater than that in the sitting position (26). Thus, the superior-inferior movement of the thoraco-abdominal organs due to respiration in the upright condition may not be as large as that observed in the supine position in the current study. The long duration of the upright scans prevented the adoption of a constant respiratory condition; as such, alternative imaging modalities may be required to test these hypotheses. Additionally, the effect of dynamic movement (e.g. running) and different task specific postures (e.g. kneeling rifle position) on organ positions is unknown.

5. Conclusions

The aim of this study was to quantify the positions of a number of important internal thoraco-abdominal organs and structures for a cohort of young male adults in different breathing conditions and postures. Significant differences in organ positioning were found between the studied scan conditions, verifying the importance of breathing and postural considerations for body armour coverage analysis.

Inspiration resulted in the most lateral organ boundaries with the exception of the heart, the left boundary of which was more laterally positioned during expiration. The upright conditions generally resulted in the most inferior organ boundaries, therefore representing the most conservative locations of these organs for body armour length analysis. The upright condition also represents a common posture adopted by police and military personnel and thus the upright data was used for an exemplar body armour coverage analysis of hard plates of common dimensions. Parametrised distributions of the upright organ boundary data have been presented for use in simple coverage analysis of existing or proposed body armour dimensions. Additionally, sufficient data has been provided for future researchers to conduct coverage analysis using the supine data or the most conservative available data for each anatomical point of interest.

The data herein may be used to establish a representative population database of thoraco-abdominal organ and anatomical structure boundary positions with respect to the studied breathing and postural conditions. Such a database will facilitate more evidence-based design and assessment of the coverage afforded by body armour.

References

1. Peoples G, Silk A, Notley S, Holland L, Collier B, Lee D. The effect of a tiered body armour system on soldier physical mobility. University of Wollongong: Centre for Human and Applied Physiology, Faculty of Health and Behavioural Sciences, 2010 UOW-HPL-Report-041.
2. Dempsey PC, Handcock PJ, Rehrer NJ. Impact of police body armour and equipment on mobility. Applied Ergonomics. 2013;44(6):957-61.
3. Watson CH, Horsfall, I., Fenne, P. Ergonomics of Body Armour. Personal Armour Systems Symposium Quebec City, Canada, 13-17 September 2010.
4. HOSDB. Body Armour Standards for UK Police Part 1: General Requirements. Sandridge, UK: Home Office Scientific Development Branch; 2007.
5. NIJ. Stab Resistance of Personal Body Armor NIJ Standard-0115.00 Washington, DC, USA: U.S. Department of Justice 2000.
6. Breeze J, Lewis EA, Fryer R, Hepper AE, Mahoney PF, Clasper JC. Defining the essential anatomical coverage provided by military body armour against high energy projectiles. Journal of the Royal Army Medical Corps. 2015;162(4):284-90.
7. Breeze J, Lewis EA, Fryer R. Determining the dimensions of essential medical coverage required by military body armour plates utilising Computed Tomography. Injury. 2016;47(9):1932-8.
8. Beillas P, Lafon Y, Smith FW. The effects of posture and subject-to-subject variations on the position, shape and volume of abdominal and thoracic organs. Stapp car crash journal. 2009;53:127-54.
9. Rhyne AC, Gayzik FS, Moreno DP, Stitzel JD. Methods for comparison of abdominal organ location and shape in the supine and upright positions. Biomed Sci Instrum. 2012;48:351-8.
10. Hayes AR, Gayzik FS, Moreno DP, Martin RS, Stitzel JD. Abdominal Organ Location, Morphology, and Rib Coverage for the 5(th), 50(th), and 95(th) Percentile Males and Females in the Supine and Seated Posture using Multi-Modality Imaging. Annals of Advances in Automotive Medicine. 2013;57:111-22.
11. Hayes AR, Gayzik FS, Moreno DP, Martin RS, Stitzel JD. Comparison of Organ Location, Morphology, and Rib Coverage of a Midsized Male in the Supine and Seated Positions. Computational and Mathematical Methods in Medicine. 2013.
12. Bleetman A, Dyer J. Ultrasound assessment of the vulnerability of the internal organs to stabbing: determining safety standards for stab-resistant body armour. Injury. 2000;31(8):609-12.
13. Edwards M, Furnell A, Coleman J, Davis S. A Preliminary Anthropometry Standard for Australian Army Equipment Evaluation. Land Division, Defence Science and Technology Group DSTO-TR-3006, 2014.
14. Tomkinson G, Daniell, N., Dale, M., Bowler, T. Australian Warfighter Anthropometry Survey (AWAS): Landmarking and Measurement Manual. Sansom Institute for Health Research, University of South Australia, 2012.
15. Benjamini Y, Yekutieli D. The Control of the False Discovery Rate in Multiple Testing under Dependency. The Annals of Statistics. 2001;29(4):1165-88.

16. NIJ. Selection and Application Guide to Ballistic-Resistant Body Armor for Law Enforcement, Corrections and Public Safety: NIJ Selection and Application Guide 0101.06. Washington, DC, USA: U.S. Department of Justice; 2014.
17. Ball WS, Wicks JD, Mettler FA. Prone-supine change in organ position: CT demonstration. American Journal of Roentgenology. 1980;135(4):815-20.
18. Brandner ED, Wu A, Chen H, Heron D, Kalnicki S, Komanduri K, et al. Abdominal organ motion measured using 4D CT. International Journal of Radiation Oncology, Biology, Physics. 2006;65(2):554-60.
19. Bussels B, Goethals L, Feron M, Bielen D, Dymarkowski S, Suetens P, et al. Respiration-induced movement of the upper abdominal organs: a pitfall for the three-dimensional conformal radiation treatment of pancreatic cancer. Radiotherapy and Oncology. 2003;68(1):69-74.
20. Giraud P, Yorke E, Ford EC, Wagman R, Mageras GS, Amols H, et al. Reduction of organ motion in lung tumors with respiratory gating. Lung Cancer. 2006;51(1):41-51.
21. Jagsi R, Moran JM, Kessler ML, Marsh RB, Balter JM, Pierce LJ. Respiratory Motion of The Heart and Positional Reproducibility Under Active Breathing Control. International Journal of Radiation Oncology, Biology, Physics. 2007;68(1):253-8.
22. Gatzoulis MA. Thorax. In: Standring S, editor. Gray's Anatomy: The Anatomical Basis of Clinical Practice. 40th ed: Churchill Livingstone/Elsevier; 2008.
23. Laing S, Jaffrey M. Thoraco-abdominal anatomical reference data for vulnerability models: Comparing the Visible Human to a larger sample of males. Personal Armour Systems Symposium; Amsterdam, The Netherlands, 19-23 September 2016.
24. Zygote solid 3D male anatomy colleciton generation II development report American Fork, UT 84003: Zygote Media Group Inc.
25. Laing S, Jaffrey M. A pilot study comparing the thoraco-abdominal anatomical data of the Visible Human Project Female to three living females. Personal Armour Systems Symposium; Washington, USA, 1-5 October 2018.
26. Takazakura R, Takahashi M, Nitta N, Murata K. Diaphragmatic motion in the sitting and supine positions: Healthy subject study using a vertically open magnetic resonance system. Journal of Magnetic Resonance Imaging. 2004;19(5):605-9.

Appendix A Intra- and Inter-rater variability

All anatomical points were digitised by the same person (Digitiser 1). Reliability checks were conducted to assess intra- and inter-digitiser consistency amongst the authors. The recumbent inspiration scans of two participants were assessed for intra- and inter-rater reliability (Table A-1). For each point, only the coordinate (X- or Y-) relevant to the subsequent analysis was assessed in this way. For the 27 points included in this analysis, 95% of the intra-rater absolute differences were less than 2.6 mm and 3.5 mm for Digitisers 1 and 2, respectively and 95% of all inter-rater absolute differences were less than 3.5 mm. Thus, the identification and digitising of all scans was performed by Digitiser 1.

Table A-1 *Intra- and Inter-rater reliability test statistics describing the absolute differences in the measured locations of digitised points for recumbent inspiration and upright scans. Data consolidated from a number of data set comparisons (n) where each data set consisted of the 27 anatomical points for analysis. All absolute difference values in mm.*

	Intra-rater variability						Inter-rater variability					
	n	Mean	SD	50th %ile	95th %ile	Max.	n	Mean	SD	50th %ile	95th %ile	Max.
Recumbent scans												
Digitiser 1	2	0.9	1.1	0.9	2.6	5.3	8	1.0	1.2	0.9	3.5	7.9
Digitiser 2	2	0.8	1.1	0.4	3.5	5.3						
Upright scans												
Digitiser 1	2	2.0	2.0	1.4	6.3	9.6						

Due to the lower resolution of the upright scans, an intra-rater variability assessment was completed on the upright scans of two participants (Table A-1). As a result of the lower level of confidence in the digitised points of the upright scans, a number of points of interest were repeated during the digitising process. These repeated points comprised the organ boundaries of the heart, liver, spleen and kidneys. The original and repeated points were then compared for consistency, with an acceptance threshold of 3 mm; for points within 3 mm of each other, the mean value was used in the analysis and for points with > 3 mm disparity, the point was digitised for a third time and the median value used in the analysis. The consistency was generally within the 3 mm threshold and the third measurement was only required for 9.1% of the digitised points. This level of repeatability should be considered when assessing the magnitude of differences in anatomical locations between the upright and expiration recumbent conditions presented in this report.

Appendix B Recumbent expiration data

Expiration (n=23)																
	Point #	X-coordinates (Mediolateral)					Y-coordinates (Superoinferior)					Z-coordinates (Anteroposterior)				
		Mean	SD	Min	Median	Max	Mean	SD	Min	Median	Max	Mean	SD	Min	Median	Max
Sternal Notch		0.0	0.0	0.0	0.0	0.0	0.0	0.0	0.0	0.0	0.0	0.0	0.0	0.0	0.0	0.0
Pubic symphysis (linea alba when no pelvic scan)		0.0	0.0	0.0	0.0	0.0	551.7	41.9	456.4	562.6	621.7	15.1	12.2	-5.4	14.9	47.3
SN fiduciary marker centre	1	1.9	2.7	-7.0	2.2	5.7	-0.1	0.3	-0.7	0.0	0.5	-8.1	1.9	-12.2	-7.7	-5.0
Left common carotid artery (lateral boundary) at height of SN fiduciary marker centre	2	20.7	3.6	14.9	21.0	27.1	-0.2	0.3	-0.7	-0.1	0.6	39.5	7.0	26.1	39.2	56.3
Left subclavian artery (lateral boundary) at height of SN fiduciary marker centre	3	30.1	3.6	24.5	29.3	37.6	-0.2	0.4	-0.8	-0.2	0.8	54.2	8.5	36.9	54.9	77.4
Left brachiocephalic vein (lateral boundary) at height of SN fiduciary marker centre	4	37.6	6.7	18.8	38.1	47.7	-0.2	0.5	-1.0	-0.3	0.7	28.4	3.9	20.3	28.8	36.9
Most lateral lungs at height of SN fiduciary marker centre (left)	5	96.4	10.9	80.1	96.7	115.5	-0.3	1.2	-1.8	-0.5	2.8	77.3	8.2	66.6	76.1	93.6
Brachiocephalic trunk (lateral boundary) at height of SN fiduciary marker centre	6	-10.9	7.4	-28.4	-10.9	0.4	-0.1	0.3	-0.8	0.0	0.7	31.0	3.9	22.5	31.5	38.3
Right brachiocephalic vein (lateral boundary) at height of SN fiduciary marker centre	7	-43.2	4.7	-53.8	-43.7	-31.9	0.1	0.7	-1.8	0.1	1.4	29.4	4.8	18.5	29.7	39.6
Most lateral lungs at height of SN fiduciary marker (right)	8	-94.7	9.6	-116.8	-93.2	-80.1	0.1	1.3	-3.9	0.0	2.1	77.0	8.9	60.3	77.0	94.5
Anatomical SN	9	0.1	0.3	-0.5	0.1	0.6	8.0	6.1	-5.7	7.9	26.2	8.3	2.3	4.5	8.1	12.2
Manubriosternal joint centre	10	0.6	2.6	-4.3	0.6	4.7	58.1	7.3	45.1	56.4	73.5	-11.7	5.2	-21.6	-11.7	-2.7
Anatomical xiphisternal joint centre	11	3.6	4.7	-7.9	3.2	11.3	172.3	12.3	142.6	175.0	195.1	-20.5	10.9	-38.3	-20.7	2.7
Xiphisternal joint fiduciary marker centre	12	6.7	4.9	-3.6	6.2	16.0	174.6	12.8	154.8	175.4	206.5	-41.6	11.2	-61.7	-40.1	-20.7
Tip of xiphoid process	13	5.4	5.2	-5.5	5.1	14.5	203.2	17.0	174.2	201.3	237.5	-20.3	11.7	-40.1	-22.1	4.9
L5-S1 (centre intervertebral disc)	14	-0.3	4.5	-11.4	0.3	8.8	431.0	24.5	380.6	425.3	473.4	73.1	7.4	54.0	74.3	86.0
L4-L5 (centre intervertebral disc)	15	0.6	4.6	-6.9	0.0	9.1	394.1	24.3	353.4	389.4	445.4	62.9	8.1	49.5	64.8	78.8
L3-L4 (centre intervertebral disc)	16	0.9	4.5	-8.8	-0.3	9.3	355.3	23.3	318.1	350.9	403.4	64.3	9.0	47.7	65.7	78.8
L2-L3 (centre intervertebral disc)	17	0.5	4.4	-10.8	1.0	7.3	317.9	22.2	280.5	313.3	362.2	70.8	10.1	49.1	72.5	87.8
L1-L2 (centre intervertebral disc)	18	0.2	4.0	-12.7	1.1	5.7	282.0	21.2	245.5	278.3	322.9	78.8	9.8	59.9	81.5	95.4
T12-L1 (centre intervertebral disc)	19	0.2	3.6	-12.0	1.2	4.6	247.4	20.1	212.2	244.2	286.1	85.0	9.6	67.1	87.3	102.6
T11-T12 (centre intervertebral disc)	20	0.6	3.3	-10.4	1.6	4.6	213.5	18.1	181.6	210.9	251.1	90.8	9.4	76.1	92.3	109.4
T10-T11 (centre intervertebral disc)	21	0.8	3.3	-7.9	1.8	5.3	183.5	17.3	152.7	182.0	219.6	94.6	9.1	79.2	94.5	113.0
T9-T10 (centre intervertebral disc)	22	0.5	3.9	-7.1	1.0	5.6	155.4	16.4	125.5	153.2	188.1	96.4	8.7	79.2	97.2	113.0
T8-T9 (centre intervertebral disc)	23	-0.1	4.4	-8.2	0.1	5.3	128.8	15.7	99.3	126.9	159.3	97.3	8.6	79.2	98.1	113.0
T7-T8 (centre intervertebral disc)	24	-0.7	4.8	-10.9	-0.8	5.9	103.5	15.1	75.6	101.6	131.3	97.6	8.2	79.2	98.1	109.8
T6-T7 (centre intervertebral disc)	25	-1.1	4.7	-12.8	-0.8	5.6	78.8	14.6	52.9	76.6	105.4	96.1	8.3	79.2	96.3	109.8
T5-T6 (centre intervertebral disc)	26	-1.1	4.3	-11.2	-0.6	5.9	55.3	14.0	30.1	52.6	81.8	92.5	8.0	77.0	90.9	104.9

Expiration (n=23)																
	Point #	X-coordinates (Mediolateral)					Y-coordinates (Superoinferior)					Z-coordinates (Anteroposterior)				
		Mean	SD	Min	Median	Max	Mean	SD	Min	Median	Max	Mean	SD	Min	Median	Max
T4-T5 (centre intervertebral disc)	27	-0.4	3.8	-9.0	-0.5	6.1	32.5	13.6	10.0	31.9	59.9	86.9	8.2	71.6	87.3	101.3
T3-T4 (centre intervertebral disc)	28	0.1	3.2	-7.3	0.0	5.5	11.0	12.9	-10.1	9.6	38.1	79.4	8.4	66.2	78.3	95.9
T2-T3 (centre intervertebral disc)	29	0.0	3.2	-7.0	-0.1	5.9	-8.8	12.3	-28.0	-9.6	17.9	69.7	8.9	56.7	68.0	88.7
T1-T2 (centre intervertebral disc)	30	-0.8	3.1	-8.8	-0.1	3.7	-28.2	12.5	-48.1	-28.4	-0.4	59.1	9.5	44.6	57.6	79.7
C7-T1 (centre intervertebral disc)	31	-1.8	3.2	-9.6	-1.8	4.4	-46.2	12.5	-65.6	-46.8	-20.6	48.1	10.1	30.2	46.4	70.7
L5 left most lateral border of vertebral body	32	28.3	4.1	20.9	28.2	35.9	412.1	24.3	365.3	408.6	457.5	68.2	7.6	50.4	68.4	84.2
L5 right most lateral border of vertebral body	33	-27.7	5.1	-36.9	-28.3	-16.8	412.7	24.5	366.2	410.0	457.7	68.2	7.6	50.4	68.4	84.2
T10 left most lateral border of vertebral body	34	21.8	4.1	13.0	22.0	27.6	171.8	18.4	141.5	166.2	209.8	95.9	9.3	79.2	96.3	113.0
T10 right lateral border of vertebral body	35	-20.6	3.4	-29.0	-20.5	-14.9	171.8	18.2	141.1	165.8	210.2	95.9	9.3	79.2	96.3	113.0
T1 left most lateral border of vertebral body	36	15.9	3.6	5.3	15.9	21.0	-38.9	13.2	-59.5	-39.8	-11.8	54.3	10.1	37.4	53.1	76.1
T1 right most lateral border of vertebral body	37	-17.9	3.7	-28.9	-17.1	-13.1	-38.4	13.1	-59.5	-39.4	-12.7	54.3	10.1	37.4	53.1	76.1
Spinous Process L5	38	0.2	5.0	-10.7	0.1	11.1	404.5	22.9	363.5	406.9	439.7	126.5	7.3	112.5	126.9	141.8
Spinous Process L3	39	-0.2	4.5	-8.9	-0.9	12.2	349.2	22.1	310.6	349.1	386.7	132.7	9.5	113.0	133.2	152.6
Spinous Process L1	40	-0.3	4.9	-14.4	-0.2	9.2	277.5	20.7	244.6	275.7	317.6	143.0	9.8	121.5	142.2	165.6
Spinous Process T10	41	1.4	3.8	-9.7	1.9	7.1	186.5	16.8	155.3	183.8	225.8	149.7	9.9	132.3	150.3	168.8
Spinous Process T7	42	0.5	4.9	-8.2	2.0	7.8	111.0	18.2	79.6	108.6	144.8	150.2	9.6	133.2	148.5	171.0
Spinous Process T3	43	-0.8	3.8	-9.1	-0.4	5.7	-5.2	16.2	-31.1	-3.1	23.2	129.6	10.0	112.5	126.9	153.5
Spinous Process T2	44	-0.4	3.5	-6.6	0.0	5.7	-30.6	15.0	-54.2	-30.6	-3.5	118.0	10.0	98.1	117.0	142.7
Spinous Process C7	45	-1.8	3.8	-10.5	-2.1	5.4	-70.8	12.5	-92.4	-70.0	-45.5	95.0	10.4	77.0	95.4	117.0
Umbilicus/Omphalion fiduciary marker	46	1.5	4.2	-10.0	1.3	11.4	377.9	19.0	344.7	382.3	410.4	-30.8	11.7	-48.2	-30.6	-2.3
10th rib fiduciary marker (left)	47	149.5	21.6	113.8	151.0	189.1	333.2	15.7	291.1	335.4	350.9	41.2	29.9	-11.3	41.4	84.6
Iliocristale fiduciary marker (left)	48	162.9	11.3	143.2	159.3	186.1	370.7	22.6	313.9	371.9	409.7	71.0	14.1	45.0	70.7	103.1
Iliocristale (left)	49	115.2	16.0	79.9	117.0	137.1	391.3	19.7	344.1	390.5	423.1	71.0	14.1	45.0	70.7	103.1
Anterior superior iliac spine (left)	50	115.6	10.5	92.8	113.8	136.0	456.9	23.3	414.8	457.0	510.0	2.0	10.0	-16.2	-0.5	18.9
10th Rib fiduciary marker (right)	51	-144.9	24.1	-177.8	-148.2	-99.8	336.2	19.5	291.3	337.7	383.8	35.7	30.4	-11.7	32.9	82.8
Iliocristale fiduciary marker (right)	52	-161.8	11.3	-180.7	-160.9	-143.8	373.8	22.0	332.0	377.1	409.4	72.7	11.8	45.5	72.5	92.3
Iliocristale (right)	53	-112.6	12.5	-130.2	-115.8	-79.3	391.2	21.7	345.8	392.1	421.2	72.7	11.8	45.5	72.5	92.3
Anterior superior iliac spine (right)	54	-116.7	9.4	-130.8	-117.8	-89.1	458.9	24.6	420.7	458.2	522.1	1.8	10.9	-17.1	1.8	19.8
10th Rib (left) most inferior boundary	55	118.0	11.8	91.0	119.1	142.3	323.7	17.3	288.4	330.0	350.0	22.7	13.4	-2.7	24.8	51.3
10th Rib (right) most inferior boundary	56	-114.8	10.8	-131.5	-115.3	-86.6	322.5	17.7	285.3	322.7	353.7	21.0	11.4	-5.0	20.3	47.7
Thelion fiduciary marker (left)	57	118.2	9.8	104.0	118.4	134.5	144.3	11.2	130.9	141.7	168.2	-32.1	13.0	-53.6	-33.8	-4.1
Left lateral border of the ribcage (serratus anterior) at thelion level	58	157.0	7.4	137.9	157.7	176.4	144.3	11.0	131.0	141.9	168.2	61.1	11.1	40.5	61.2	79.2
Left lateral border of the ribcage (serratus anterior)	59	159.8	8.0	139.2	161.1	178.6	178.2	27.1	128.4	184.0	224.9	61.6	11.8	32.4	61.7	87.8
Left lung most lateral	60	136.8	7.6	115.5	138.9	150.2	160.9	27.1	92.0	170.2	206.8	60.5	12.3	38.7	57.6	85.5
Thelion fiduciary marker (right)	61	-103.4	8.9	-118.4	-102.4	-89.0	148.0	13.5	120.1	148.8	176.6	-32.9	12.0	-52.2	-32.0	-9.5
Right lateral border of the ribcage (serratus anterior) at thelion level	62	-155.2	6.6	-166.6	-155.0	-139.8	148.1	13.5	120.9	148.6	176.5	68.7	12.7	50.4	69.3	91.4

Expiration (n=23)																
	Point #	X-coordinates (Mediolateral)					Y-coordinates (Superoinferior)					Z-coordinates (Anteroposterior)				
		Mean	SD	Min	Median	Max	Mean	SD	Min	Median	Max	Mean	SD	Min	Median	Max
Right lateral border of the ribcage (serratus anterior)	63	-157.5	7.6	-170.5	-158.2	-142.7	180.1	28.2	130.0	183.6	229.1	64.0	12.6	43.2	65.3	91.4
Right lung most lateral	64	-133.3	6.4	-145.1	-133.4	-120.0	152.2	22.1	110.1	154.2	197.4	66.4	12.3	44.1	64.4	96.8
Left lung most superior	65	42.4	5.5	33.3	43.2	56.9	-38.3	10.2	-63.9	-36.7	-15.4	68.0	6.5	53.6	68.9	81.5
Right lung most superior	66	-43.4	4.6	-53.0	-43.0	-35.5	-36.9	9.8	-64.8	-35.0	-17.0	66.3	7.9	51.3	65.3	81.9
Left lung anterior surface (left lung only)	67	62.0	11.8	37.9	59.4	84.8	140.7	40.6	81.7	135.9	202.1	-13.9	8.3	-27.9	-15.8	-0.9
Left lung posterior surface (left lung only)	68	71.1	7.9	53.3	71.4	83.9	124.2	23.4	86.3	123.4	171.6	138.6	10.1	114.3	140.4	159.8
Left cardiac border (lateral boundary)	69	102.6	9.7	89.7	100.4	124.9	150.2	13.3	124.6	146.7	174.7	19.6	9.4	2.7	18.9	42.8
Left atrial 'bulge' (superolateral boundary)	70	39.6	6.9	29.9	38.7	54.7	49.9	11.8	28.9	49.7	73.0	30.2	6.5	18.0	31.1	42.8
Left ventricular 'bulge' (superolateral boundary)	71	77.8	8.7	58.1	77.6	96.6	93.2	15.6	61.8	92.9	124.5	39.4	7.0	24.3	39.6	51.8
Right cardiac border (lateral boundary)	72	-44.5	6.5	-59.0	-44.0	-29.8	116.4	15.3	84.3	112.7	141.8	29.4	7.2	15.3	27.9	41.9
Inferior cardiac border	73	60.5	11.2	34.1	61.2	83.8	190.1	14.9	159.1	191.5	214.6	-2.8	8.8	-18.9	-4.5	14.0
Superior aortic border (aortic arch)	74	20.4	6.6	8.8	20.1	33.7	6.3	7.3	-11.6	7.5	22.3	52.3	6.8	34.7	53.1	61.7
Left aortic border (lateral border of aortic arch/upper descending aorta)	75	41.3	5.0	31.5	41.0	50.3	26.6	8.8	7.9	28.3	44.1	70.2	5.7	60.3	71.1	80.6
Right border of superior vena cava (Right-most border of SVC near the union of the contra-lateral brachiocephalic veins)	76	-36.4	5.6	-45.7	-35.9	-27.4	47.2	10.6	27.6	48.1	70.1	42.9	4.0	36.5	41.9	50.0
Pulmonary artery left (first bifurcation)	77	53.7	3.7	47.2	53.7	63.6	45.8	9.7	24.6	44.7	61.8	72.3	6.3	58.1	72.9	82.8
Pulmonary artery right (first bifurcation)	78	-25.4	5.1	-34.3	-25.2	-14.0	58.0	10.7	40.1	56.4	80.4	58.2	4.4	50.4	58.5	66.6
Anterior boundary of heart	79	45.7	19.0	13.3	49.7	75.0	153.3	15.1	120.8	153.2	183.3	-14.9	7.7	-30.2	-14.4	0.9
Posterior boundary of aorta	80	25.8	5.2	16.7	24.0	35.6	93.0	14.4	72.8	91.9	128.6	100.8	5.8	91.4	100.8	113.0
Celiac trunk (inferior point of celiac trunk before bifurcation)	81	15.5	5.3	3.1	16.1	24.3	245.0	17.6	216.1	244.5	287.8	48.1	10.9	23.9	50.0	65.3
Left renal artery origin on aorta (inferior point)	82	17.1	5.1	2.7	17.6	24.7	276.7	16.6	241.2	276.9	318.4	54.4	10.2	31.1	52.7	70.2
Right renal artery origin on aorta (inferior point)	83	1.1	5.2	-11.9	0.9	9.8	274.6	16.9	238.8	273.9	307.1	49.5	10.2	25.7	49.1	63.0
Abdominal aorta bifurcation point into common iliac arteries	84	6.5	5.3	-6.4	6.7	17.5	379.9	19.8	328.7	385.1	428.7	35.6	9.7	14.9	37.8	51.8
Union of common iliac veins to inferior vena cava	85	-10.5	6.3	-29.1	-7.9	-2.2	412.0	18.9	364.1	414.0	460.3	45.9	9.2	28.8	45.9	64.4
Left boundary of liver (lateral)	86	84.4	21.5	52.0	79.9	126.1	183.8	18.8	138.8	180.0	213.6	24.8	19.2	-7.2	24.8	70.2
Right boundary of liver (lateral)	87	-138.9	7.4	-152.9	-140.1	-125.1	224.8	22.8	177.9	229.0	256.5	69.6	11.1	47.7	68.4	96.8
Most superior right lobe of liver	88	-77.9	10.7	-98.9	-79.7	-56.6	134.4	21.5	88.9	132.0	178.1	55.4	11.2	21.2	56.7	73.8
Most inferior right lobe of liver	89	-113.5	11.8	-132.8	-112.6	-92.8	319.0	23.7	270.2	324.8	352.7	60.9	15.3	30.6	61.2	90.9
Common hepatic artery (most inferior point)	90	7.1	9.3	-8.9	7.3	23.0	247.4	17.9	217.2	244.6	291.3	41.0	11.4	20.3	38.7	61.2
Most lateral point of inferior vena cava within liver	91	-42.3	5.8	-53.9	-42.2	-32.3	218.1	24.5	175.6	216.8	271.4	66.7	9.3	49.1	67.1	82.4

Expiration (n=23)																
	Point #	X-coordinates (Mediolateral)					Y-coordinates (Superoinferior)					Z-coordinates (Anteroposterior)				
		Mean	SD	Min	Median	Max	Mean	SD	Min	Median	Max	Mean	SD	Min	Median	Max
Portal vein (inferior boundary of junction of splenic vein and superior mesenteric vein)	92	7.6	6.4	-4.2	8.1	19.5	260.6	18.4	226.6	264.0	295.7	30.2	11.5	0.5	31.5	47.3
Portal vein (junction of inferior border of the portal vein and the right lobe of the liver at the coronal slice corresponding to the thickest section of the portal vein)	93	-55.5	9.5	-75.8	-56.8	-39.4	227.5	18.3	188.8	228.3	254.8	49.2	9.1	31.1	49.5	71.6
Right branch portal vein bifurcation	94	-73.2	8.2	-93.9	-73.5	-62.3	220.6	20.1	185.0	219.5	247.9	54.3	11.6	23.4	54.9	73.8
Right hepatic vein 1st union point	95	-46.7	9.5	-73.3	-45.2	-26.3	168.1	18.0	133.2	168.0	201.7	71.9	12.2	54.9	71.1	100.4
Right hepatic vein 2nd union point	96	-61.0	9.5	-84.7	-59.5	-41.3	181.5	16.4	143.0	180.8	215.8	70.1	13.1	44.1	72.0	105.8
Right hepatic vein 3rd union point	97	-73.3	11.6	-94.6	-72.0	-56.3	198.3	19.9	152.7	202.8	233.3	71.8	14.3	40.5	69.8	105.8
Left boundary of spleen (lateral)	98	139.3	9.3	116.3	140.1	155.6	217.9	21.0	179.7	214.7	264.7	69.4	13.1	49.5	66.6	98.6
Right boundary of spleen (lateral)	99	37.5	7.1	23.9	37.4	54.2	187.7	15.0	159.0	186.1	227.2	100.3	13.1	80.1	97.2	123.8
Superior boundary of spleen	100	80.7	9.5	63.7	82.8	95.2	155.5	14.0	127.4	155.9	186.5	90.6	14.2	69.3	90.9	122.0
Inferior boundary of spleen	101	116.3	11.2	81.9	120.4	131.3	262.5	23.8	215.0	262.2	310.4	94.9	18.9	60.8	92.7	124.7
Lateral hilum of spleen	102	112.1	6.4	96.9	113.6	124.2	219.8	20.8	186.1	214.1	261.7	69.9	17.4	29.3	73.4	100.8
Inferior hilum of spleen	103	105.2	7.4	88.7	104.8	119.4	230.8	19.3	197.6	230.7	263.4	75.8	18.3	37.4	78.3	105.3
Left lateral kidney border	104	104.6	7.6	87.2	106.0	123.0	270.8	21.2	236.2	269.2	331.3	103.0	11.6	71.1	102.6	123.8
Left medial kidney border superior	105	28.1	4.6	15.1	28.7	40.6	233.2	17.1	205.6	233.6	267.6	86.7	9.7	70.2	86.9	111.2
Left medial kidney border inferior	106	48.5	6.4	37.2	48.7	63.5	285.2	18.9	248.5	285.3	330.6	88.1	12.4	68.9	83.7	109.8
Left kidney superior pole	107	40.7	5.3	26.3	40.5	49.3	206.2	17.7	179.5	201.5	252.7	104.3	10.0	84.6	105.3	122.4
Left kidney inferior pole	108	74.3	8.2	60.1	72.9	96.0	321.4	19.0	292.7	319.6	370.7	92.4	11.0	74.7	94.1	113.4
Left kidney renal sinus lateral boundary	109	82.3	8.5	66.1	82.4	106.3	277.6	20.8	244.0	277.8	316.4	94.2	10.2	69.3	96.3	115.2
Left kidney renal sinus inferior boundary	110	72.7	8.4	59.7	71.6	97.7	295.4	18.9	261.2	296.4	342.7	90.4	10.1	69.3	91.4	107.1
Right lateral kidney border	111	-102.5	7.2	-115.8	-102.4	-89.2	287.4	23.7	242.5	283.5	348.6	100.3	10.7	81.0	101.3	119.7
Right medial kidney border superior	112	-28.6	5.2	-39.8	-28.4	-22.3	247.2	18.6	217.5	246.5	295.9	86.3	10.5	66.6	87.3	107.6
Right medial kidney border inferior	113	-46.0	5.9	-57.0	-45.5	-37.2	294.1	21.7	254.6	289.2	354.5	79.5	13.8	54.5	77.9	116.1
Right kidney superior pole	114	-41.9	5.3	-56.5	-41.5	-34.9	221.1	20.7	191.6	219.0	278.4	104.4	10.0	81.9	104.4	122.4
Right kidney inferior pole	115	-73.2	7.3	-86.0	-74.9	-62.6	331.3	21.6	298.8	322.2	387.0	84.6	10.2	64.8	83.3	103.5
Right kidney renal sinus lateral boundary	116	-79.9	6.8	-96.3	-79.9	-63.6	289.2	21.9	257.7	282.6	354.6	92.1	12.2	71.1	93.6	117.0
Right kidney renal sinus inferior boundary	117	-71.0	7.1	-86.3	-70.1	-60.2	304.4	20.8	266.4	296.6	359.0	85.0	10.7	66.6	84.2	103.5
Left renal artery inferior point	118	25.0	7.9	13.5	23.0	48.3	278.6	16.6	244.5	279.0	321.9	57.2	10.7	34.7	52.7	74.7
Right renal artery inferior point	119	-16.7	13.4	-45.2	-12.5	-0.3	279.2	17.2	250.5	277.8	321.2	57.2	14.3	36.0	56.3	90.0
Pancreas tail (left boundary)	120	91.8	11.7	53.1	92.2	110.0	230.0	18.9	205.2	228.9	271.0	75.7	15.0	48.6	79.2	102.2
Pancreas head (right boundary)	121	-49.1	5.1	-59.1	-48.7	-40.0	273.4	19.2	241.0	271.0	305.6	38.3	11.9	14.9	36.9	57.6
Pancreas head/uncinate process (inferior boundary)	122	-18.4	13.6	-44.8	-17.5	10.8	304.0	19.0	269.6	304.4	338.7	33.4	12.2	4.1	33.3	52.2
Pancreas uncinate process (left boundary)	123	5.0	8.3	-8.6	4.8	30.0	286.9	17.3	255.5	289.5	313.2	35.2	11.3	7.6	32.9	52.7
Pancreas head/neck junction (on superior surface vertical to point 123)	124	4.8	8.6	-9.4	4.7	29.9	233.7	18.7	197.8	230.1	273.0	27.1	13.1	-5.0	27.5	47.3
Repeat SN fiduciary marker	125	1.8	2.6	-6.1	2.2	5.7	0.1	0.3	-0.5	0.0	0.5	-8.2	2.0	-12.2	-7.7	-5.0

Expiration (n=23)															
	Point #	X-coordinates (Mediolateral)					Y-coordinates (Superoinferior)					Z-coordinates (Anteroposterior)				
		Mean	SD	Min	Median	Max	Mean	SD	Min	Median	Max	Mean	SD	Min	Median	Max
Repeat anatomical SN	126	-0.1	0.3	-0.6	0.0	0.5	7.8	6.6	-7.4	7.9	26.3	8.0	2.5	4.1	7.2	13.1
Repeat manubriosternal joint centre	127	0.2	2.1	-4.3	0.3	4.3	58.3	7.2	45.1	57.3	73.5	-11.6	5.0	-18.5	-12.6	-0.9
Repeat anatomical xiphisternal joint centre	128	3.8	4.6	-7.0	3.8	12.2	172.9	12.8	142.6	175.0	194.7	-21.0	10.6	-38.3	-21.2	0.9
Pubic symphysis (linea alba when no pelvic scan)	129	0.1	0.3	-0.5	0.0	0.4	548.3	41.9	458.6	560.9	613.4	14.7	12.9	-5.4	14.9	45.5
Repeat pubic symphysis (linea alba when no pelvic scan)	130	-0.1	0.3	-0.4	0.0	0.5	549.4	41.0	461.6	562.6	619.5	15.4	12.3	-5.4	14.9	49.1

Appendix C Recumbent inspiration data

Inspiration (n=23)																
	Point #	X-coordinates (Mediolateral)					Y-coordinates (Superoinferior)					Z-coordinates (Anteroposterior)				
		Mean	SD	Min	Median	Max	Mean	SD	Min	Median	Max	Mean	SD	Min	Median	Max
Sternal Notch		0.0	0.0	0.0	0.0	0.0	0.0	0.0	0.0	0.0	0.0	0.0	0.0	0.0	0.0	0.0
Pubic symphysis (linea alba when no pelvic scan)		0.0	0.0	0.0	0.0	0.0	551.7	41.9	456.4	562.6	621.7	19.0	15.7	-11.3	16.2	46.4
SN fiduciary marker centre	1	2.1	2.7	-6.1	3.1	6.6	0.0	0.4	-0.9	0.0	0.9	-8.5	3.0	-13.5	-9.0	-1.8
Left common carotid artery (lateral boundary) at height of SN fiduciary marker centre	2	19.9	3.7	13.1	19.3	25.8	0.0	0.5	-1.2	0.0	0.7	39.4	6.4	27.0	38.7	54.5
Left subclavian artery (lateral boundary) at height of SN fiduciary marker centre	3	27.1	3.0	21.9	27.1	33.7	0.0	0.5	-1.2	0.0	0.8	52.0	6.4	36.0	53.6	65.7
Left brachiocephalic vein (lateral boundary) at height of SN fiduciary marker centre	4	36.5	6.6	17.5	38.5	45.1	-0.1	0.6	-1.4	0.0	0.9	28.7	3.5	21.6	28.4	39.6
Most lateral lungs at height of SN fiduciary marker centre (left)	5	99.9	10.8	83.1	100.2	119.4	-0.2	1.4	-2.3	-0.3	3.2	75.9	7.9	62.1	77.0	97.2
Brachiocephalic trunk (lateral boundary) at height of SN fiduciary marker centre	6	-16.0	6.6	-32.4	-16.2	-3.9	0.1	0.5	-0.7	0.1	1.2	32.7	3.7	23.4	33.3	40.5
Right brachiocephalic vein (lateral boundary) at height of SN fiduciary marker centre	7	-41.7	4.7	-49.4	-41.6	-31.5	0.1	0.7	-1.6	0.1	1.4	28.9	4.7	18.0	28.4	39.6
Most lateral lungs at height of SN fiduciary marker (right)	8	-96.4	10.2	-118.1	-95.4	-77.9	0.3	1.4	-3.6	0.3	2.3	76.3	9.6	57.6	75.2	91.8
Anatomical SN	9	0.1	0.3	-0.4	0.0	0.9	4.9	6.5	-6.1	4.8	24.1	8.1	3.0	1.8	8.1	13.5
Manubriosternal joint centre	10	0.5	2.5	-4.2	0.3	4.4	55.2	7.7	43.3	55.6	72.2	-13.6	6.3	-27.0	-14.0	-2.3
Anatomical xiphisternal joint centre	11	3.8	4.5	-6.1	3.0	13.4	168.9	12.1	142.2	170.5	193.5	-24.3	10.3	-41.4	-23.9	-1.3
Xiphisternal joint fiduciary marker centre	12	6.7	5.0	-5.2	6.2	16.6	174.3	12.4	155.2	175.1	206.0	-44.4	11.6	-67.5	-43.7	-23.0
Tip of xiphoid process	13	5.1	5.3	-6.8	5.7	16.9	199.1	20.7	164.1	198.4	238.4	-23.7	11.6	-41.4	-23.9	0.9
L5-S1 (centre intervertebral disc)	14	-0.4	4.3	-9.7	-0.9	9.6	434.5	26.0	384.6	432.3	475.6	79.0	8.0	61.2	79.7	90.9
L4-L5 (centre intervertebral disc)	15	0.3	4.1	-7.1	0.3	9.0	397.2	25.3	355.7	395.5	445.8	69.3	8.0	52.2	69.3	84.2
L3-L4 (centre intervertebral disc)	16	0.6	4.2	-9.0	0.8	7.5	358.3	24.3	318.1	357.9	404.7	70.8	9.1	55.8	68.0	87.8
L2-L3 (centre intervertebral disc)	17	0.3	3.8	-10.9	1.1	6.0	321.1	23.1	280.4	320.3	362.7	77.6	10.1	59.4	75.2	97.2
L1-L2 (centre intervertebral disc)	18	0.0	3.8	-12.0	1.1	4.5	285.2	22.3	246.3	282.7	324.2	85.1	10.6	70.2	83.3	108.0
T12-L1 (centre intervertebral disc)	19	0.1	3.7	-10.4	1.1	4.9	250.6	21.1	212.2	247.7	287.4	92.0	10.0	77.4	90.5	115.2
T11-T12 (centre intervertebral disc)	20	0.5	3.5	-9.8	0.8	5.6	216.6	19.2	182.4	214.3	252.5	96.7	9.9	81.0	95.4	120.6
T10-T11 (centre intervertebral disc)	21	0.8	3.6	-6.4	1.4	6.2	186.5	18.3	153.6	183.7	220.1	100.4	9.5	84.6	101.3	120.6
T9-T10 (centre intervertebral disc)	22	0.9	4.1	-6.6	2.0	7.5	158.3	17.7	126.4	154.9	189.5	102.3	9.1	84.6	102.6	120.6
T8-T9 (centre intervertebral disc)	23	0.5	4.5	-7.2	2.1	6.9	131.9	16.8	101.0	129.1	160.6	103.5	9.2	86.0	103.5	122.4
T7-T8 (centre intervertebral disc)	24	-0.1	5.0	-10.9	1.5	7.3	106.5	16.4	75.7	104.6	132.6	104.0	9.4	86.0	104.0	122.4
T6-T7 (centre intervertebral disc)	25	-0.4	4.9	-11.0	1.1	6.7	81.9	15.6	52.9	80.1	107.2	102.0	10.0	80.6	102.2	122.4
T5-T6 (centre intervertebral disc)	26	-0.1	4.4	-8.5	-0.1	7.1	58.2	15.0	31.0	56.5	83.6	98.5	9.9	80.6	96.8	118.8

Inspiration (n=23)																
	Point #	X-coordinates (Mediolateral)					Y-coordinates (Superoinferior)					Z-coordinates (Anteroposterior)				
		Mean	SD	Min	Median	Max	Mean	SD	Min	Median	Max	Mean	SD	Min	Median	Max
T4-T5 (centre intervertebral disc)	27	0.3	4.2	-8.5	1.6	7.3	35.6	14.4	10.0	34.2	60.8	93.0	10.2	75.2	92.3	115.2
T3-T4 (centre intervertebral disc)	28	0.5	3.7	-6.9	0.4	6.7	14.1	13.7	-9.2	12.3	39.8	84.8	10.4	68.0	82.8	106.2
T2-T3 (centre intervertebral disc)	29	0.2	3.6	-6.9	-0.9	6.3	-6.1	13.2	-27.6	-5.7	18.8	75.6	10.7	61.2	73.4	98.6
T1-T2 (centre intervertebral disc)	30	-0.1	3.2	-6.9	-0.1	5.3	-25.2	13.0	-46.8	-26.1	-0.4	64.6	11.3	50.9	64.4	88.2
C7-T1 (centre intervertebral disc)	31	-1.1	3.0	-8.7	-1.0	4.9	-43.9	13.4	-64.3	-46.3	-18.8	54.5	10.9	39.6	53.6	79.2
L5 left most lateral border of vertebral body	32	27.7	4.0	21.8	26.6	35.2	415.7	26.2	373.5	416.9	463.2	74.2	8.5	57.6	75.2	89.6
L5 right most lateral border of vertebral body	33	-27.5	4.8	-37.7	-27.8	-17.9	415.8	26.2	374.5	417.8	463.4	74.2	8.5	57.6	75.2	89.6
T10 left most lateral border of vertebral body	34	22.0	4.3	14.2	22.3	29.2	172.1	18.0	138.0	169.4	203.4	101.4	9.3	86.4	100.8	122.4
T10 right lateral border of vertebral body	35	-19.8	3.7	-28.0	-19.1	-15.1	172.3	18.1	137.6	170.0	203.6	101.4	9.3	86.4	100.8	122.4
T1 left most lateral border of vertebral body	36	17.4	3.5	8.8	17.3	23.1	-35.9	13.2	-52.9	-38.5	-11.8	60.1	11.2	45.0	59.0	84.6
T1 right most lateral border of vertebral body	37	-17.3	3.0	-23.5	-16.9	-12.4	-35.8	13.3	-53.8	-38.5	-11.6	60.1	11.2	45.0	59.0	84.6
Spinous Process L5	38	0.1	4.6	-10.6	0.0	10.2	408.0	24.5	360.9	408.2	443.2	132.4	9.3	111.6	131.9	148.5
Spinous Process L3	39	-0.3	4.2	-8.1	-0.5	12.0	352.1	22.7	310.3	353.5	385.4	138.8	9.8	115.2	137.3	159.3
Spinous Process L1	40	-0.4	4.5	-12.9	-0.6	9.1	280.6	20.9	247.2	279.6	319.8	149.0	12.0	122.4	147.6	180.0
Spinous Process T10	41	1.5	4.2	-10.8	1.8	7.2	190.2	18.3	157.0	186.4	227.1	154.7	11.0	133.2	154.4	180.0
Spinous Process T7	42	1.2	5.3	-9.5	2.4	7.3	113.8	20.1	80.1	107.7	146.6	155.0	11.4	133.2	156.2	185.4
Spinous Process T3	43	-0.2	4.2	-7.8	-0.4	8.8	-2.1	16.9	-32.0	-3.5	29.3	133.2	12.8	113.4	131.0	165.6
Spinous Process T2	44	0.1	4.1	-8.7	-0.9	7.0	-26.9	15.9	-52.5	-28.4	2.1	123.4	11.7	100.8	122.0	147.2
Spinous Process C7	45	-1.2	3.5	-7.8	-1.3	5.0	-67.8	12.2	-90.6	-68.7	-43.3	101.0	11.3	81.0	100.4	129.6
Umbilicus/Omphalion fiduciary marker	46	1.1	4.1	-8.4	1.7	12.3	378.0	19.8	344.3	379.7	416.1	-35.4	13.9	-60.3	-34.7	-6.3
10th rib fiduciary marker (left)	47	151.7	20.1	118.5	154.8	188.1	334.8	16.8	293.1	336.7	358.4	42.8	32.5	-16.7	44.1	90.9
Iliocristale fiduciary marker (left)	48	163.2	11.1	145.6	159.5	185.9	372.8	23.8	315.0	372.5	414.9	74.8	14.6	48.6	72.5	103.1
Iliocristale (left)	49	116.2	15.5	83.9	118.3	138.0	395.9	21.1	347.9	394.6	424.7	74.9	14.6	48.6	72.5	103.1
Anterior superior iliac spine (left)	50	116.9	11.9	92.5	113.8	143.9	458.5	21.7	416.2	460.2	490.7	7.5	9.7	-7.2	6.8	25.2
10th Rib fiduciary marker (right)	51	-147.0	23.3	-180.0	-150.6	-101.2	338.1	20.6	291.5	339.8	386.2	36.6	32.8	-14.9	39.6	87.8
Iliocristale fiduciary marker (right)	52	-162.0	11.6	-182.6	-162.5	-143.9	376.0	23.5	333.4	378.8	413.9	76.2	12.9	52.2	76.1	96.3
Iliocristale (right)	53	-115.1	12.2	-130.5	-119.6	-82.3	395.2	22.8	345.1	401.4	424.5	76.2	12.9	52.2	76.1	96.3
Anterior superior iliac spine (right)	54	-118.1	12.4	-151.7	-117.6	-89.5	459.8	22.3	420.9	461.6	496.4	7.5	10.8	-10.8	7.6	23.4
10th Rib (left) most inferior boundary	55	125.1	10.9	99.2	124.8	148.5	320.0	17.9	286.9	323.8	347.1	23.9	12.8	-1.8	24.8	52.7
10th Rib (right) most inferior boundary	56	-122.6	11.3	-143.3	-122.4	-89.8	318.3	18.3	279.4	318.5	353.3	22.9	9.7	5.4	21.6	40.1
Thelion fiduciary marker (left)	57	119.2	9.5	105.0	118.5	136.8	145.5	11.9	132.0	145.0	176.2	-34.7	13.3	-59.0	-37.4	-2.7
Left lateral border of the ribcage (serratus anterior) at thelion level	58	159.6	8.0	136.4	161.1	177.4	145.5	11.8	132.1	145.1	176.2	63.2	12.6	37.8	65.7	84.6
Left lateral border of the ribcage (serratus anterior)	59	162.7	8.6	138.5	163.0	180.6	177.4	20.7	140.0	181.7	202.6	65.7	15.1	37.8	65.7	99.5
Left lung most lateral	60	144.1	9.7	114.8	145.4	158.6	191.0	31.0	109.2	196.3	231.0	61.9	14.6	34.2	59.0	92.7
Thelion fiduciary marker (right)	61	-104.1	9.0	-122.5	-103.4	-90.8	149.5	13.2	120.6	149.3	177.4	-35.7	12.3	-57.2	-32.4	-15.3
Right lateral border of the ribcage (serratus anterior) at thelion level	62	-157.7	6.8	-168.7	-158.4	-142.3	149.6	13.2	121.6	149.6	177.3	65.6	14.2	44.1	65.3	93.6

Inspiration (n=23)																
	Point #	X-coordinates (Mediolateral)					Y-coordinates (Superoinferior)					Z-coordinates (Anteroposterior)				
		Mean	SD	Min	Median	Max	Mean	SD	Min	Median	Max	Mean	SD	Min	Median	Max
Right lateral border of the ribcage (serratus anterior)	63	-160.3	8.2	-178.4	-160.5	-143.5	181.2	25.3	126.0	184.2	228.7	64.5	12.4	44.1	64.4	90.0
Right lung most lateral	64	-140.9	7.3	-152.1	-140.9	-126.0	192.9	25.5	132.3	194.5	225.7	68.4	12.9	45.0	68.9	94.1
Left lung most superior	65	43.8	6.2	34.6	42.2	56.3	-36.8	10.1	-62.2	-35.6	-15.3	70.0	8.2	59.9	69.8	90.0
Right lung most superior	66	-43.1	5.2	-56.1	-42.0	-35.0	-36.0	10.5	-64.7	-33.7	-16.2	67.2	8.7	47.3	66.2	81.0
Left lung anterior surface (left lung only)	67	61.7	14.5	31.4	62.0	92.0	157.2	38.5	85.8	156.1	244.2	-20.5	9.9	-39.6	-18.5	-0.9
Left lung posterior surface (left lung only)	68	73.1	8.4	49.9	76.3	84.9	136.5	32.0	83.3	131.3	209.4	145.8	10.3	117.0	145.8	165.6
Left cardiac border (lateral boundary)	69	92.4	8.5	80.6	90.0	115.4	169.4	16.1	136.5	167.5	202.0	18.2	13.9	-12.6	20.3	45.9
Left atrial 'bulge' (superolateral boundary)	70	36.0	5.8	25.4	36.0	45.3	65.0	12.2	36.7	63.3	90.4	31.8	8.1	16.2	31.1	47.7
Left ventricular 'bulge' (superolateral boundary)	71	73.4	7.3	54.6	72.6	82.8	117.8	16.9	76.3	117.8	149.8	36.2	9.0	21.2	36.5	54.9
Right cardiac border (lateral boundary)	72	-44.1	6.9	-59.1	-44.5	-26.9	135.4	15.7	96.1	138.0	163.2	30.6	9.3	9.0	31.1	49.5
Inferior cardiac border	73	52.3	9.8	30.3	52.5	68.8	208.3	15.6	173.5	211.9	236.5	-1.1	10.2	-19.8	-2.3	18.0
Superior aortic border (aortic arch)	74	19.3	5.0	6.2	20.2	28.7	16.5	8.6	-3.7	15.3	31.9	56.0	6.6	39.6	59.0	68.4
Left aortic border (lateral border of aortic arch/upper descending aorta)	75	37.8	4.0	30.6	37.7	45.6	36.5	10.3	12.2	37.0	54.7	74.3	8.1	60.3	72.0	91.8
Right border of superior vena cava (Right-most border of SVC near the union of the contra-lateral brachiocephalic veins)	76	-32.2	6.5	-44.2	-32.3	-21.7	57.3	14.7	24.7	60.0	92.5	43.7	5.8	30.6	44.1	53.6
Pulmonary artery left (first bifurcation)	77	51.2	5.2	44.4	50.8	61.8	58.8	10.7	30.4	60.2	79.5	73.4	8.8	49.5	73.8	85.1
Pulmonary artery right (first bifurcation)	78	-28.0	5.3	-39.5	-26.3	-16.1	72.2	11.7	47.5	74.8	95.9	58.7	6.3	41.4	60.8	66.2
Anterior boundary of heart	79	44.1	13.2	18.3	45.8	63.9	171.8	19.8	127.5	170.1	205.9	-16.9	9.2	-34.2	-17.1	2.3
Posterior boundary of aorta	80	23.2	3.9	16.5	22.0	33.6	97.1	14.8	74.0	96.9	137.7	102.5	8.2	87.3	102.2	120.6
Celiac trunk (inferior point of celiac trunk before bifurcation)	81	14.4	4.7	3.5	16.6	19.8	255.3	19.9	222.7	254.6	294.4	48.1	11.5	27.9	46.4	75.6
Left renal artery origin on aorta (inferior point)	82	17.0	4.3	5.4	18.0	22.4	283.4	17.7	246.0	284.8	322.4	60.0	11.4	41.4	58.5	84.2
Right renal artery origin on aorta (inferior point)	83	0.8	4.9	-10.4	0.5	9.6	281.2	17.2	241.9	279.1	308.4	55.1	10.6	37.8	51.8	75.6
Abdominal aorta bifurcation point into common iliac arteries	84	6.8	4.7	-2.9	7.9	16.2	385.3	20.2	332.7	389.4	425.6	41.0	8.5	25.2	40.5	56.7
Union of common iliac veins to inferior vena cava	85	-10.6	6.2	-22.6	-9.5	2.1	415.9	20.7	371.6	420.3	464.2	50.1	9.5	32.4	50.0	69.3
Left boundary of liver (lateral)	86	83.1	19.3	45.5	75.1	126.5	214.0	18.8	166.4	213.4	243.5	14.0	20.8	-18.0	14.4	73.8
Right boundary of liver (lateral)	87	-142.6	7.7	-156.5	-144.4	-127.8	235.7	22.3	185.5	238.4	270.4	69.4	11.7	46.8	68.0	92.7
Most superior right lobe of liver	88	-73.5	17.5	-108.6	-76.4	-24.5	169.2	22.5	109.4	168.4	209.7	49.5	16.7	10.8	48.2	79.2
Most inferior right lobe of liver	89	-110.1	10.7	-129.0	-109.7	-90.9	353.1	29.5	291.5	356.7	408.6	49.3	18.1	9.0	51.8	88.7
Common hepatic artery (most inferior point)	90	4.3	10.8	-15.3	8.1	19.3	261.8	17.8	227.9	265.3	297.0	39.2	10.5	23.4	39.2	63.9
Most lateral point of inferior vena cava within liver	91	-42.7	5.7	-57.4	-41.3	-34.1	238.9	29.4	192.9	235.8	287.7	64.7	13.0	36.0	62.6	88.2

Inspiration (n=23)																
	Point #	X-coordinates (Mediolateral)					Y-coordinates (Superoinferior)					Z-coordinates (Anteroposterior)				
		Mean	SD	Min	Median	Max	Mean	SD	Min	Median	Max	Mean	SD	Min	Median	Max
Portal vein (inferior boundary of junction of splenic vein and superior mesenteric vein)	92	11.7	8.3	-3.4	11.3	25.6	277.3	20.5	240.2	279.0	313.1	30.7	11.3	10.8	29.3	53.6
Portal vein (junction of inferior border of the portal vein and the right lobe of the liver at the coronal slice corresponding to the thickest section of the portal vein)	93	-54.3	9.7	-75.8	-53.7	-37.7	256.0	21.5	202.9	256.8	286.6	44.4	12.3	7.2	44.6	62.1
Right branch portal vein bifurcation	94	-72.7	8.4	-93.6	-71.9	-54.3	252.8	22.3	202.1	253.0	287.7	50.2	12.5	31.5	48.2	75.6
Right hepatic vein 1st union point	95	-51.9	9.3	-77.2	-52.0	-29.3	200.6	21.6	150.3	198.1	240.3	69.1	15.6	43.2	66.2	101.7
Right hepatic vein 2nd union point	96	-62.3	10.1	-87.6	-60.4	-47.3	213.8	21.8	155.6	217.1	262.7	66.7	17.6	39.6	66.6	112.5
Right hepatic vein 3rd union point	97	-76.3	13.5	-94.1	-75.3	-54.1	230.1	22.4	177.6	229.9	276.7	67.3	18.3	38.3	63.0	112.5
Left boundary of spleen (lateral)	98	142.0	9.0	118.1	142.2	162.3	246.1	23.3	199.5	245.8	282.8	70.3	12.9	52.2	67.5	110.3
Right boundary of spleen (lateral)	99	41.5	8.1	30.2	40.3	59.0	215.5	19.5	164.8	219.1	247.6	99.0	14.6	77.4	95.0	128.7
Superior boundary of spleen	100	81.9	9.9	58.6	80.4	106.7	187.0	18.8	139.2	183.8	220.4	85.4	17.3	50.4	82.8	119.7
Inferior boundary of spleen	101	117.2	8.5	97.3	119.2	131.3	291.5	27.8	237.9	286.8	330.2	88.8	19.6	55.4	84.2	124.7
Lateral hilum of spleen	102	112.5	7.6	98.5	113.0	130.0	246.7	21.8	211.7	243.8	288.8	67.5	17.4	37.8	66.6	101.3
Inferior hilum of spleen	103	104.9	7.5	92.3	105.1	125.5	259.8	22.5	220.5	254.5	291.5	74.9	17.6	39.2	75.2	105.3
Left lateral kidney border	104	107.2	7.4	91.3	108.3	125.7	297.6	23.7	255.5	303.3	335.0	101.6	13.7	68.4	103.1	126.0
Left medial kidney border superior	105	31.3	4.8	22.0	31.7	42.3	252.0	22.1	215.7	254.1	285.7	89.7	12.2	70.2	89.6	115.2
Left medial kidney border inferior	106	51.6	6.4	41.1	50.5	68.6	307.4	21.4	265.6	310.9	338.9	85.3	15.8	60.3	88.7	114.3
Left kidney superior pole	107	44.1	6.1	32.3	42.8	55.8	230.1	20.4	196.3	230.4	263.6	107.1	10.7	90.0	105.8	133.2
Left kidney inferior pole	108	77.1	8.1	65.6	74.8	97.9	344.1	22.4	305.5	347.3	382.4	89.8	13.6	67.1	90.5	111.6
Left kidney renal sinus lateral boundary	109	85.1	8.5	72.2	86.4	109.0	298.2	23.8	259.0	301.4	339.2	94.1	12.5	68.4	95.4	117.0
Left kidney renal sinus inferior boundary	110	75.5	7.5	64.3	73.8	92.5	316.9	23.3	277.0	319.7	355.3	89.0	12.5	67.1	89.1	109.8
Right lateral kidney border	111	-103.4	7.1	-114.8	-105.0	-89.3	317.3	25.5	267.5	317.6	368.9	95.9	12.5	77.0	92.7	121.1
Right medial kidney border superior	112	-32.5	6.0	-45.9	-30.8	-25.5	269.5	24.1	228.4	273.7	320.9	84.8	12.6	63.0	84.6	112.1
Right medial kidney border inferior	113	-47.7	5.7	-57.5	-47.7	-37.3	319.4	22.4	283.2	325.2	365.0	70.3	18.8	41.4	66.6	117.5
Right kidney superior pole	114	-45.0	4.5	-57.4	-43.3	-39.2	249.6	25.2	210.7	251.1	301.9	103.9	9.6	86.4	101.7	126.0
Right kidney inferior pole	115	-73.8	7.5	-88.8	-71.5	-62.2	357.6	25.5	318.6	360.1	405.9	74.7	14.9	46.4	77.0	104.9
Right kidney renal sinus lateral boundary	116	-80.3	6.9	-96.0	-79.2	-66.5	315.5	23.2	272.3	313.3	357.3	86.8	12.9	64.4	88.2	113.9
Right kidney renal sinus inferior boundary	117	-71.4	7.6	-87.3	-70.6	-59.0	331.4	26.8	287.9	339.0	383.6	76.3	14.5	48.2	77.0	104.9
Left renal artery inferior point	118	35.4	10.0	16.1	36.3	53.0	288.1	19.1	250.1	290.4	325.8	66.9	13.2	48.6	63.5	98.1
Right renal artery inferior point	119	-26.2	11.4	-47.9	-27.5	-1.8	292.6	18.7	258.4	295.3	335.8	64.9	12.2	46.8	61.2	92.7
Pancreas tail (left boundary)	120	92.8	12.9	55.0	94.8	114.1	257.0	21.7	216.2	254.3	290.9	73.6	15.7	45.0	72.5	106.2
Pancreas head (right boundary)	121	-43.1	8.7	-59.8	-41.6	-27.3	298.5	22.2	255.3	301.0	332.1	33.2	12.5	9.9	32.4	60.3
Pancreas head/uncinate process (inferior boundary)	122	-17.1	13.6	-40.7	-18.7	9.5	324.9	20.9	279.8	329.9	359.0	32.0	10.8	12.6	29.3	50.4
Pancreas uncinate process (left boundary)	123	7.9	8.1	-2.3	8.3	28.7	302.7	20.0	263.9	306.7	331.5	36.4	12.2	14.4	33.8	57.2
Pancreas head/neck junction (on superior surface vertical to point 123)	124	7.7	8.3	-2.5	8.4	27.9	255.2	19.6	209.6	256.4	289.7	24.4	12.2	6.8	25.2	49.5
Repeat SN fiduciary marker	125	2.2	2.7	-6.1	3.1	6.6	-0.1	0.4	-0.9	0.0	0.9	-8.5	3.2	-13.5	-9.0	0.0

Inspiration (n=23)															
	Point #	X-coordinates (Mediolateral)					Y-coordinates (Superoinferior)					Z-coordinates (Anteroposterior)				
		Mean	SD	Min	Median	Max	Mean	SD	Min	Median	Max	Mean	SD	Min	Median	Max
Repeat anatomical SN	126	0.0	0.4	-0.9	0.0	0.5	4.5	6.9	-10.1	4.8	24.9	8.8	3.5	0.0	8.6	13.5
Repeat manubriosternal joint centre	127	0.6	2.4	-3.4	0.7	4.9	55.3	7.5	43.3	55.6	72.2	-13.6	5.8	-27.0	-14.4	-5.0
Repeat anatomical xiphisternal joint centre	128	3.8	4.9	-7.8	4.0	13.4	169.3	11.5	141.8	169.8	192.9	-23.6	10.2	-41.4	-24.8	-1.3
Pubic symphysis (linea alba when no pelvic scan)	129	0.0	0.2	-0.4	0.0	0.5	551.8	41.9	461.7	562.2	621.7	18.4	15.2	-16.7	18.0	47.3
Repeat pubic symphysis (linea alba when no pelvic scan)	130	0.0	0.2	-0.5	0.0	0.4	551.6	42.0	451.2	563.1	621.7	19.6	16.7	-14.4	15.8	45.9

Appendix D Upright data

Upright (n=14)																
	Point #	X-coordinates (Mediolateral)					Y-coordinates (Superoinferior)					Z-coordinates (Anteroposterior)				
		Mean	SD	Min	Median	Max	Mean	SD	Min	Median	Max	Mean	SD	Min	Median	Max
Sternal Notch		0.0	0.0	0.0	0.0	0.0	556.4	41.1	456.4	564.6	621.7	-32.7	22.2	-95.1	-28.1	0.0
Pubic symphysis (linea alba when no pelvic scan)		1.4	2.8	-4.1	1.0	8.2	0.0	0.4	-0.7	0.0	1.0	-8.1	3.3	-14.1	-7.9	-1.8
SN fiduciary marker centre	1	18.9	2.5	13.7	19.1	24.6	-0.2	0.6	-1.0	-0.3	0.8	33.0	7.3	21.0	32.5	52.6
Left common carotid artery (lateral boundary) at height of SN fiduciary marker centre	3	26.4	3.5	19.1	28.0	30.1	-0.3	0.7	-1.3	-0.4	1.0	45.0	9.0	28.0	45.5	66.7
Left subclavian artery (lateral boundary) at height of SN fiduciary marker centre	5	97.9	11.0	76.6	98.4	118.3	-1.4	2.5	-4.7	-1.6	3.7	78.1	9.4	63.4	78.9	94.7
Lungs: Most lateral left at height of SN fiduciary marker centre	6	-18.2	4.9	-26.0	-18.1	-9.6	0.3	0.7	-0.5	0.3	1.7	31.5	6.2	21.0	31.7	45.6
Brachiocephalic trunk (lateral boundary) at height of SN fiduciary marker centre	8	-94.4	10.7	-114.2	-90.5	-80.7	1.4	2.5	-3.3	2.2	5.2	77.1	9.7	59.6	77.3	94.5
Lungs: Most lateral right at height of SN fiduciary marker	9	0.1	0.4	-1.0	0.1	0.9	1.5	5.4	-8.2	2.7	9.1	8.9	2.9	3.5	9.6	14.1
Anatomical SN	10	0.9	2.6	-2.2	0.3	7.5	53.3	7.5	42.4	52.6	67.9	-12.7	7.4	-24.5	-14.0	0.0
Manubriosternal joint centre	11	2.2	3.7	-6.8	3.7	6.0	161.5	8.6	139.4	161.4	173.9	-29.7	13.1	-45.9	-32.4	-7.1
Anatomical xiphisternal joint centre	12	5.5	4.1	-2.7	7.5	10.4	169.7	19.6	143.4	166.2	226.5	-50.3	16.5	-73.6	-49.9	-21.2
Xiphisternal joint fiduciary marker centre	14	-1.0	6.5	-11.5	-3.1	10.1	429.1	25.5	385.4	433.2	462.3	86.9	23.3	31.7	91.4	122.8
L5-S1 (centre intervertebral disc)	15	0.1	8.0	-14.7	-1.1	15.9	392.7	23.9	351.7	393.3	421.1	81.6	23.3	24.6	86.6	115.8
L4-L5 (centre intervertebral disc)	16	1.3	9.1	-11.1	1.6	16.2	353.5	22.3	312.1	353.6	381.0	81.1	21.3	31.7	84.9	115.8
L3-L4 (centre intervertebral disc)	17	1.1	9.3	-9.0	-0.1	17.8	315.2	20.9	273.7	316.3	341.7	84.6	21.6	38.7	86.0	122.8
L2-L3 (centre intervertebral disc)	18	1.3	9.4	-9.2	-0.5	16.9	278.8	19.7	236.8	281.3	306.0	88.6	20.4	52.8	89.5	122.8
L1-L2 (centre intervertebral disc)	19	1.2	8.2	-7.7	-1.6	14.0	244.2	18.5	204.0	247.0	269.0	94.6	19.7	63.0	94.9	136.8
T12-L1 (centre intervertebral disc)	20	1.4	7.9	-9.9	-0.3	14.4	211.3	17.3	172.5	212.7	234.8	98.6	19.1	70.0	98.4	136.8
T11-T12 (centre intervertebral disc)	21	1.1	7.0	-10.8	2.3	12.0	181.0	16.8	142.3	181.8	203.3	99.1	17.2	70.0	100.0	136.8
T10-T11 (centre intervertebral disc)	22	0.7	6.3	-10.3	2.7	10.3	153.0	16.8	113.6	153.0	179.1	99.6	15.0	77.0	100.0	129.8
T9-T10 (centre intervertebral disc)	23	0.9	5.6	-9.6	1.1	9.9	125.8	16.0	86.2	126.3	148.9	100.1	15.2	75.2	101.9	129.8
T8-T9 (centre intervertebral disc)	24	0.7	5.2	-8.9	1.0	9.6	99.9	14.9	61.5	101.3	120.1	100.6	12.6	82.2	101.9	122.8
T7-T8 (centre intervertebral disc)	25	0.5	5.1	-9.6	0.3	9.3	74.9	14.7	35.5	76.8	94.1	101.1	11.2	82.2	101.9	122.8
T6-T7 (centre intervertebral disc)	26	1.3	4.8	-7.5	0.9	9.0	50.7	13.7	13.7	52.3	68.1	97.1	12.1	77.0	96.5	122.8
T5-T6 (centre intervertebral disc)	27	1.8	4.4	-5.6	1.5	8.7	28.8	13.0	-8.2	29.9	44.9	90.1	10.5	77.0	91.2	110.2
T4-T5 (centre intervertebral disc)	28	2.5	4.1	-4.9	2.8	9.4	7.3	12.0	-26.0	9.7	20.2	81.1	10.4	70.0	77.3	103.2
T3-T4 (centre intervertebral disc)	29	2.1	3.6	-4.1	2.5	8.8	-13.7	11.9	-45.1	-10.3	-0.4	74.1	10.6	59.5	70.5	96.2
T2-T3 (centre intervertebral disc)	30	0.8	3.2	-4.0	0.9	8.0	-32.1	12.0	-61.6	-31.2	-14.4	62.5	12.1	45.5	61.5	88.0
C7-T1 (centre intervertebral disc)	31	-0.3	2.8	-4.6	-0.1	7.4	-50.4	12.0	-79.3	-47.6	-35.5	53.5	9.6	38.5	49.4	73.9
L5 left most lateral border of vertebral body	32	27.6	8.4	10.8	25.4	39.7	411.6	26.0	367.3	413.3	444.6	85.6	22.0	31.7	88.4	115.8

Upright (n=14)																
	Point #	X-coordinates (Mediolateral)					Y-coordinates (Superoinferior)					Z-coordinates (Anteroposterior)				
		Mean	SD	Min	Median	Max	Mean	SD	Min	Median	Max	Mean	SD	Min	Median	Max
L5 right most lateral border of vertebral body	33	-28.3	7.2	-39.7	-30.8	-10.9	410.8	23.3	372.4	413.3	441.1	85.6	22.0	31.7	88.4	115.8
T10 left most lateral border of vertebral body	34	21.4	6.4	11.2	21.3	34.1	166.7	16.6	129.5	167.9	190.8	101.1	16.2	77.0	100.1	136.8
T10 right most lateral border of vertebral body	35	-19.7	7.2	-31.6	-19.4	-10.1	166.9	16.7	130.6	168.0	192.0	101.1	16.2	77.0	100.1	136.8
T1 left most lateral border of vertebral body	36	16.4	2.9	11.4	16.0	23.5	-42.9	13.2	-75.6	-42.9	-26.4	56.5	10.6	42.0	56.2	75.2
T1 right most lateral border of vertebral body	37	-16.1	3.8	-21.7	-16.5	-6.6	-42.1	13.3	-74.8	-41.4	-25.6	56.5	10.6	42.0	56.2	75.2
Spinous Process L5	38	-1.1	6.6	-9.7	-1.4	13.4	412.1	27.9	362.1	413.8	448.7	137.7	21.8	102.1	142.3	171.9
Spinous Process L3	39	-1.2	7.9	-11.1	0.5	12.9	344.1	22.6	297.2	347.2	369.1	140.7	24.1	102.1	142.2	178.9
Spinous Process L1	40	-0.9	7.4	-11.2	-3.9	12.5	271.2	19.9	232.9	271.1	302.1	145.7	22.3	105.0	145.7	185.9
Spinous Process T10	41	0.5	6.2	-9.7	2.4	10.6	183.7	18.0	143.8	180.2	216.0	153.8	19.4	119.0	151.5	193.0
Spinous Process T7	42	1.4	9.5	-13.2	2.0	13.9	115.4	12.1	102.3	114.5	133.4	148.6	11.3	131.2	149.7	161.0
Umbilicus/Omphalion fiduciary marker	46	1.1	3.7	-6.3	0.5	7.4	369.0	20.6	347.9	362.7	418.3	-57.8	18.8	-95.1	-57.8	-31.5
10th rib fiduciary marker (left)	47	157.1	9.6	147.4	154.4	175.2	336.9	21.3	304.2	335.5	388.8	56.3	23.4	10.6	61.2	101.5
Iliocristale fiduciary marker (left)	48	162.2	8.4	152.3	159.3	178.1	371.7	29.5	330.6	378.0	412.5	68.6	21.6	31.7	73.9	101.5
Iliocristale (left)	49	126.8	13.3	111.4	129.7	157.7	403.9	29.5	360.7	410.3	440.3	68.6	21.6	31.7	73.9	101.5
10th Rib fiduciary marker (right)	51	-150.0	10.4	-162.9	-150.0	-133.5	330.5	16.7	304.0	333.8	351.9	48.3	18.4	21.0	40.2	80.5
Iliocristale fiduciary marker (right)	52	-159.1	9.9	-173.4	-159.1	-135.9	367.5	31.0	317.8	373.5	406.5	70.0	19.8	42.0	77.4	101.5
Iliocristale (right)	53	-127.9	13.2	-142.6	-128.9	-96.6	398.4	23.6	349.3	404.2	425.5	69.3	19.5	42.0	75.2	101.5
Left lung most lateral	60	137.4	9.9	117.9	141.5	148.7	156.8	33.9	109.3	151.5	241.7	55.0	19.9	21.0	53.5	101.7
Right lung most lateral	64	-133.7	8.9	-151.0	-133.1	-116.1	162.3	30.4	100.8	163.5	225.4	59.0	14.1	35.0	57.1	87.7
Left lung - most superior	65	44.0	5.9	35.6	43.7	58.8	-37.4	8.0	-54.0	-37.9	-24.6	70.6	8.8	56.3	70.9	87.7
Right lung - most superior	66	-41.2	4.9	-49.7	-41.4	-34.8	-34.9	7.9	-48.8	-34.9	-19.0	70.1	8.5	56.3	69.1	87.7
Left lung anterior surface (left lung only)	67	47.9	9.1	28.4	49.2	61.1	111.3	18.7	80.1	113.5	149.4	-15.2	11.1	-31.5	-17.5	3.5
Left lung posterior surface (left lung only)	68	72.4	7.8	52.6	73.4	82.2	116.5	21.1	83.1	119.4	150.7	138.8	17.7	105.0	140.5	171.9
Left cardiac border (lateral boundary)	69	95.1	10.5	77.4	95.3	111.7	182.2	18.3	161.3	178.4	228.4	8.9	15.2	-14.0	6.2	35.3
Left atrial 'bulge' (superolateral boundary)	70	38.1	6.4	23.7	38.3	47.5	83.2	14.1	69.5	80.6	120.2	18.2	13.2	0.0	16.6	42.3
Left ventricular 'bulge' (superolateral boundary)	71	76.6	7.6	63.7	78.1	86.4	128.4	16.5	111.0	122.9	164.2	22.9	15.0	3.5	20.2	45.9
Right cardiac border (lateral boundary)	72	-43.4	6.6	-54.8	-44.5	-29.0	146.7	17.9	122.6	144.2	187.0	18.4	15.2	-3.5	19.3	49.4
Inferior cardiac border	73	57.7	14.4	25.2	60.3	80.7	218.2	19.3	192.0	215.6	267.1	-2.6	16.1	-29.8	-4.4	24.6
Superior aortic border (aortic arch)	74	18.7	5.2	9.5	20.4	24.1	20.8	7.4	2.1	22.0	30.2	48.0	8.0	35.2	45.7	66.7
Left aortic border (lateral border of aortic arch/upper descending aorta)	75	35.6	4.5	29.1	35.0	42.2	36.7	7.6	20.9	37.7	47.5	62.5	7.1	47.2	63.0	73.7
Anterior boundary of heart	79	52.3	17.0	4.3	54.4	75.8	179.5	25.1	140.4	179.1	243.1	-19.7	14.5	-38.7	-21.9	3.5
Posterior boundary of aorta	80	18.6	5.2	8.8	18.9	27.0	83.4	27.8	38.5	74.1	123.6	86.1	8.8	75.2	84.2	105.8
Left renal artery origin on aorta (inferior point)	82	20.0	9.7	7.7	15.9	36.6	283.3	20.8	248.7	284.3	337.1	56.3	20.5	10.6	56.3	82.2
Right renal artery origin on aorta (inferior point)	83	3.8	9.3	-9.2	1.4	19.0	278.3	19.4	253.9	278.2	323.9	51.9	20.1	3.5	52.9	75.2
Abdominal aorta bifurcation point into common iliac arteries	84	8.7	8.2	-3.3	8.5	25.8	380.0	26.5	323.3	380.3	440.9	49.5	23.5	-3.5	52.7	87.7
Left boundary of liver (lateral)	86	83.6	18.7	58.3	81.7	125.8	233.5	27.2	191.4	232.9	279.6	-4.6	21.7	-45.8	-3.5	31.6

Upright (n=14)																
	Point #	X-coordinates (Mediolateral)					Y-coordinates (Superoinferior)					Z-coordinates (Anteroposterior)				
		Mean	SD	Min	Median	Max	Mean	SD	Min	Median	Max	Mean	SD	Min	Median	Max
Right boundary of liver (lateral)	87	-134.6	10.2	-147.2	-135.8	-111.2	239.8	23.3	209.1	237.0	289.6	58.8	15.9	31.5	60.5	84.7
Most superior right lobe of liver	88	-72.1	16.2	-98.4	-73.9	-40.9	171.4	23.3	138.6	165.4	222.6	36.7	18.3	10.6	35.2	66.5
Most inferior right lobe of liver	89	-95.0	17.3	-117.4	-98.2	-54.2	366.9	25.8	318.1	366.5	418.7	39.7	27.5	0.0	30.7	87.7
Left boundary of spleen (lateral)	98	133.9	10.2	115.8	137.1	146.9	242.3	25.3	202.2	242.5	291.1	64.3	14.8	42.0	64.1	91.7
Superior boundary of spleen	100	84.2	10.3	63.1	84.4	100.8	184.9	22.8	156.1	178.7	232.1	74.1	18.9	52.5	70.0	115.8
Inferior boundary of spleen	101	109.3	6.9	91.2	109.5	119.4	309.6	29.5	263.6	300.1	369.3	74.3	21.1	40.2	71.9	108.8
Left lateral kidney border	104	106.4	7.2	92.4	104.7	118.0	315.2	33.0	277.1	310.6	401.0	83.1	28.4	10.6	92.2	122.8
Left medial kidney border superior	105	36.1	8.5	23.0	33.9	49.4	265.1	28.5	232.1	255.1	344.5	79.3	26.4	17.6	85.9	110.2
Left medial kidney border inferior	106	50.9	7.2	39.2	49.1	64.7	317.1	28.7	285.1	312.5	394.9	73.6	29.8	0.0	78.1	115.8
Left kidney superior pole	107	47.0	9.3	36.1	45.8	64.4	237.3	26.4	199.2	227.0	295.2	94.9	17.9	59.9	95.2	120.0
Left kidney inferior pole	108	76.9	9.0	61.8	77.3	94.1	353.6	29.5	316.8	351.2	430.8	71.0	33.7	-10.6	79.0	115.8
Right lateral kidney border	111	-98.1	10.6	-112.2	-102.4	-76.8	317.9	46.9	247.5	305.9	416.1	82.4	27.2	3.5	82.3	115.5
Right medial kidney border superior	112	-31.0	13.8	-59.7	-31.0	-10.3	276.3	48.1	212.4	262.1	373.1	71.4	26.0	17.6	77.5	112.9
Right medial kidney border inferior	113	-39.2	14.5	-59.4	-41.9	-15.2	323.4	42.6	264.1	316.6	419.7	61.1	29.4	-21.1	70.4	88.2
Right kidney superior pole	114	-46.3	13.5	-68.6	-44.7	-26.7	253.8	52.0	176.7	237.2	364.1	89.2	20.7	45.8	92.7	119.0
Right kidney inferior pole	115	-66.5	13.7	-83.7	-66.8	-47.5	360.8	44.9	288.1	346.0	452.9	58.7	32.7	-28.2	64.8	105.0
Left renal artery inferior point	118	32.4	17.9	-13.4	36.8	54.5	288.3	24.2	255.9	285.0	351.8	55.3	24.4	0.0	52.9	80.6
Right renal artery inferior point	119	-19.4	16.0	-45.4	-14.8	4.0	290.8	29.6	264.0	282.3	368.9	54.1	22.9	3.5	60.0	77.6
Repeat SN fiduciary marker	125	1.4	2.4	-3.6	1.1	6.8	-0.1	0.5	-1.0	0.0	0.7	-8.6	2.7	-14.1	-8.8	-3.5
Repeat anatomical SN	126	-0.1	0.4	-1.0	0.0	0.4	3.3	7.5	-8.2	2.8	19.9	7.9	3.4	1.8	7.0	14.1
Tracheal bifurcation (carina)	131	-1.7	3.6	-7.3	-1.8	5.0	60.6	8.8	50.3	57.1	84.5	56.0	8.1	42.0	54.5	73.7
Linea alba	132	0.0	0.0	0.0	0.0	0.0	453.6	24.3	404.0	453.8	491.5	-32.7	22.2	-95.1	-28.1	0.0

DEFENCE SCIENCE AND TECHNOLOGY GROUP DOCUMENT CONTROL DATA	1. DLM/CAVEAT (OF DOCUMENT)

2. TITLE	3. SECURITY CLASSIFICATION (FOR UNCLASSIFIED LIMITED RELEASE USE (U/L) NEXT TO DOCUMENT CLASSIFICATION)
Thoraco-abdominal Organ Locations: Variations due to Breathing and Posture and Implications for Body Armour Coverage Assessments	Document (U) Title (U) Abstract (U)
4. AUTHOR(S) Sheridan Laing and Mark Jaffrey	5. CORPORATE AUTHOR Defence Science and Technology Group 506 Lorimer St Fishermans Bend, Victoria 3207 Australia

6a. DST GROUP NUMBER	6b. AR NUMBER	6c. TYPE OF REPORT	7. DOCUMENT DATE
DST-Group-TR-3636		Technical Report	August 2019

8.TASK NUMBER	9.TASK SPONSOR	10. RESEARCH DIVISION
07/351	Diggerworks	Land Division

11. MSTC	12. STC
Land Human Systems	Physical Ergonomics

13. SECONDARY RELEASE STATEMENT OF THIS DOCUMENT

Approved for public release.

OVERSEAS ENQUIRIES OUTSIDE STATED LIMITATIONS SHOULD BE REFERRED THROUGH DOCUMENT EXCHANGE, PO BOX 1500, EDINBURGH, SA 5111

14. DELIBERATE ANNOUNCEMENT

No limitations

15. CITATION IN OTHER DOCUMENTS

Yes

16. RESEARCH LIBRARY THESAURUS

Body Armour, Protection, Anatomy, Posture

17. ABSTRACT

Body armour provides protection to the vital organs and structures of the thorax and abdomen against ballistic, stab and fragmentation threats. The positions of the organs and structures determine the coverage requirements and hence the required dimensions of body armour. The aim of this study was to quantify thoraco-abdominal organ and structure boundaries for varied breathing and postural conditions and develop a database of thoraco-abdominal organ and structure boundaries for use in body armour coverage analyses. This Technical Report documents the methodological details of the study and reports the descriptive statistics of the anatomical data. The data herein shows the necessity for consideration of breathing and postural conditions which can substantially affect the required dimensions of body armour coverage. The data may be used to establish a preliminary representative population database of thoraco-abdominal anatomical structure boundary positions with respect to the studied breathing and postural conditions. Such a database will facilitate more evidence-based design and assessment of the coverage afforded by body armour.